DIELECTRIC PROPERTIES OF PFN-PFT SOLID SOLUTION SYNTHESIZED BY THE MOLTEN SALT METHOD

by

Kazushi Amanuma

Report submitted to the Faculty of the
Virginia Polytechnic Institute and State University
in partial fulfillment of the requirements for the degree of

MASTER OF ENGINEERING

in

Materials Engineering

APPROVED:

S.B.Desu, Adviser

C.R.Houska

A.L.Ritter

August, 1991

Blacksburg, Virginia

Acknowledgement

I would like to express great appreciation to Dr.S.B.Desu, Dr.C.R.Houska, and Dr.A.L.Ritter for their reviewing this report and suggestions.

I would also like to appreciate all the faculties and students in our laboratory, especially Mr.C.C.Chiu and Mr.J.K.Chen. Without their help, I could not complete this project.

Finally, I express my deepest thanks to my family and my friends for their support and encouragement.

Table of Contents

1. Introduction

For the past 40 years, the primary materials utilized for multilayer ceramic capacitors have been modified $BaTiO_3$ and various other titanates. Such materials generally require high firing temperatures (>1300°C), making it necessary to use expensive internal electrode metals such as Pd. The upper limit of the dielectric constant for modified $BaTiO_3$ is about 4000, which determines the size of capacitors. Thus there is a high demand for a material which has a higher dielectric constant and is amenable to sintering at lower temperatures.

Lead complex oxides $Pb(B_1,B_2)O_3$, which show perovskite structure, are of considerable interest because of its high dielectric constant, broad maxima, and relatively low firing temperature. However such materials are difficult to fabricate reproducibly without the appearance of pyrochlore phases whose absence are detrimental to the dielectric properties.

Lead ferroniobate $Pb(Fe_{0.5}Nb_{0.5})O_3$ (PFN) is one of such lead perovskite oxides. The Curie temperature of PFN is 114°C and it has a high dielectric constant around 114°C. On the other hand, $Pb(Fe_{0.5}Ta_{0.5})O_3$ (PFT) has Curie point at -40°C. It is known that Curie temperature of the solid solution of PFN and PFT changes almost linearly with composition [1]. Thus the system PFN-PFT ($Pb(Fe_{0.5}Nb_{0.5})O_3$- $Pb(Fe_{0.5}Nb_{0.5})O_3$) is a potential candidate for a ceramic capacitor owing to the Curie temperature of these oxides, and to their high dielectric constants of 20,000 and 9000, respectively. An

investigation of this system has shown the existance of a solid solution with dielectric constants ranging from 6000 to 12,000. However sintering such a composition is difficult because of the refractory character of PFT.

Pure PFN was synthesized by C.Chiu and S.S.Lopatin et al. using a molten salt method.[2,3] Molten salt synthesis is one of the simplest techniques to prepare pure stoichiometric ceramic powders of multicomponent ceramic oxides. In this method, a molten salt is used as a medium of reaction of the starting oxides. Since the diffusivities of oxides in the molten salt are much higher than those in the solid-state, significantly lower powder formation temperatures and times are needed for the molten salt method.

The objective of this project is to synthesize PFN-PFT solid solutions using a molten salt method, and to obtain a foundamental knowledge about the relation among process parameters, the structure and the properties.

2.Literature Review

2.1 Molten Salt Synthesis

In the solid-state synthesis, the reaction is generally controlled by the solid-state diffusion across the inter-particle contacts. Since the diffusion takes long time to be completed, it is very difficult to obtain a completely homogeneous product in this process. In practice, the product from the first solid-state reaction is milled, and reacted again at high temperatures. This process may be repeated several times to attain homogenity but it raises the milling cost and may cause contamination due to the wear of the milling media.

On the other hand, the molten salt method can avoid these problems. The mobility of oxides in molten salts is much higher than those in the solid-state. Thus reactions can be completed much faster in the molten salt method.

The requirements of the molten salt solvent are that it not enter into any undesirable side reactions with either the reactants or the products, and that the salt should possess sufficient aqueous solubility so that it can be removed by simple washing. One solvent system which has been found to satisfy all these requirements is NaCl-KCl. This system has a eutectic at 50 mol% KCl (m.p. 931K) which dectates the minimum reaction temperature.

Reaction in the molten salt consists of two processes: complex oxide formation and particle growth.

The control of the nucleation rate is rather difficult because complex oxide particles are formed in the presence of solid reactant particles and the product usually nucleates on the reactant particles. On the other hand, growth rate can be controlled by sellecting preparation conditions, such as salt species, heating temperature and duration. Preparations of powders which have definite morphology have been reported[4,5,6].

The difficulty in synthesizing perovskite oxides is in avoiding the formation of pyrochlore phase. In the formation of PFN, the reaction takes two stages;

$$3PbO+2Nb_2O_5 \longrightarrow Pb_3Nb_4O_{13} \quad \text{(rapid)}$$
$$Pb_3Nb_2O_{13}+2Fe_2O_3+5PbO \longrightarrow 8Pb(Fe_{0.5}Nb_{0.5})O_3 \quad \text{(slow)}$$

Rasing reaction temperature and adding excess PbO can displace the equilibrium toward the perovskite phase and avoid formation of $Pb_3Nb_4O_{13}$ (P3N4)[1,2].

2.2 The Structure and the Properties of PFN and PFT

The investigation of phase transitions of PFN and PFT is still in progress. At room temperature, the crystal system of PFN is rhombohedral which is very close to cubic. A phase transition from rhombohedral (ferroelectric) to cubic (paraelectric) takes place in the range from 96°C to 120°C. PFT shows a first order phase transition from rhombohedral to monoclinic at -68°C, and a second order transition from monoclinic to cubic at -25°C.[7] The lattice constants at room temperature are

PFN	4.013 A	[8]
PFT	4.011 A	[9]

Both materials are antiferromagnetic at low temperature, but there is a considerable discrepancy among reported Neel temperatures. The Neel temperature of PFN is in the range from -264°C to -118°C. That of PFT is reported to be -130°C.[7]

B-site cations (Fe,Nb and Fe,Ta) are completely disordered in both compounds. There are two reasons for this disorder. Firstly the difference of the charges of B-site ions, Fe(+3) and Nb,Ta(+5), is not so large. If there is a larger difference of the valence between B-site cations, it results in a very srong tendency to order through electrostatic forces. Secondly the size of B-site ions are very close. If there is a large size difference in the B-site cations, materials are driven strongly towards ordering by electric forces. The ionic radii of these ions given by Ahrens [9] are

Fe	0.628 A
Nb	0.69 A
Ta	0.68 A

The stability of perovskite is estimated by two factors: tolerance factor and electronegativity difference between cations and oxygen. The tolerance factor is defined by

$$t=(r_A+r_O)/\sqrt{2}(r_B+r_O)$$

t should be from 0.88 to 1.09 for a stable perovskite

structure. Ionic radii of lead and oxygen are

Pb	1.20 A	[9]
O	1.40 A	[10]

Using these figures, the calculated tolerance factors of PFN and PFT are 0.89 and 0.90, respectively. The electronegativities of each ions given by Pauling[10] are shown in Table 1. The electronegativity difference is expressed in the following equation:

$$(X_{A-O}+X_{B-O})/2$$

where X_{A-O} is the electronegativity difference between the A site cation and oxygen, and X_{B-O} is that between the B site cations and oxygen. Since the ionic bonding gives more stable perovskite structure, the higher value of electronegativity difference is preferred. The calculated electronegativity difference of PFN and PFT are 1.75 and 2.0, respectively. From these factors, the stability of PFN and PFT are almost same.

2.3 Relaxor Ferroelectrics

Relaxor ferroelectrics are characterized by a diffuse and dispersive phase transition. The permitivity (ε') and tan δ ($\varepsilon''/\varepsilon'$) vs. temperature shows a diffuse phase transition over a so-called Curie range. There is a Curie maximum temperature, which is frequency dependent over a wide frequency range, and increases in temperature with increasing frequency. Also, the maximum in the permitivity (ε') does not correspond with the maximum in

Table 1 Electronegativity

Element	Electronegativity
Pb	1.8
Fe	1.8
Nb	1.6
Ta	1.5
O	3.5

the dielectric loss (tan δ). A model of relaxor ferroelectrics was given by Somolenski[11], which notes that ferroelectric relaxors have common characteristics where two or more cations occupy equivalent crystallographic sites. It is the distribution of these cations which gives rise to chemical microregions with various compositions and in turn differing Curie temperatures. The summed distribution of chemical microregion gives the broad phase transitions.

Thus the impurities, vacancies or composition fluctuations have to be frozen in fixed positions in the lattice for the broad phase transition. If the randomness is homogeneous, a sharp transition can occur even in systems with frozen impurities. For this reason, most of the diffuse phase transitions studied in oxide ferroelectrics have occured at low temperatures (<400°C) where the disorder is likely to be frozen. One should not expect to find diffuse phase transitions at high temperatures where the defects are more mobile in the lattice. Indeed, the sharp transitions are observed in $LiNbO_3$ and $LiTaO_3$ despite fairly large deviation from stoichiometry.

Lead perovskite oxides were classified by C.A.Randall and A.S.Bhalla based on B cation order using TEM.[12] In their study, there is a strong relation between the nanoscale or short coherent long-range B-site order and relaxtor ferroelectric behavior. PFT and PFN, which do not have any long range order of B site ions, are classified as normal ferroelectric based on its X-ray, optical, and D.T.A. study[13], even though these

compounds have a broad ferroelectric transition.

The microvolume region which has a definite Curie temperature is called a Kanzig region. A statistical treatment was developed by Rolov to describe this phenomena[14]. Assume that $Po(t,\theta)$ is the spontaneous polarization at the temperature t of the region of the crystal where the local Curie temperature lies in the range $d\theta$. Then the square of the total spontaneous polarization is given by

$$P_O^2(t) = \int F(\theta) P_O^2(t,\theta)\, d\theta \qquad (1)$$

where $F(\theta)$ is the probability density. In a solid solution of $AB'O_3$ and $AB''O_3$, the probability P(m) of observing m ions of B' in the Kanzig region of n B-site ions is given by

$$P(m) = (n!/m!(n-m)!)p^m(1-p)^n \qquad (2)$$

where p is the macroscopic concentration of B'. This distribution can be replaced by Gaussian distribution:

$$P(x) = [2\pi p(1-p)n]^{-1/2} \exp[-nx^2/2p(1-p)] \qquad (3)$$

where x=m/n-p gives the amount by which the microscopic concentration differs from the macrocsopic concentration. For small values of x, the change in Curie temperature is linearly dependent on the composition change;

$$x = g(Tc-\theta) \qquad (4)$$

The spontaneous polarization and the dielectric constant are given by (See Appendix B) ;

$$Ps^2=(c/2d)(-1-(1+4bd(T-T_0)/c^2)^{1/2}) \quad (T<Tc) \qquad (11)$$

$$Ps^2=0 \quad (T>Tc)$$

$$\varepsilon^{-1}=(c^2/d)(1+(1-4bd(T-T_0)/c^2)^{1/2})-4b(T-T_0) \quad (T<Tc) \qquad (12)$$

$$\varepsilon^{-1}=b(T-T_0) \quad (T>Tc)$$

where

$$T_0=Tc-3c^2/(16bd) \qquad (13)$$

Substituting these formulas into Eq.(1) gives the total value of each quantities.

On the other hand, it is known that the dielectric constant of relaxors obeys the law $1/\varepsilon=A+B(T-T_c)^2$ rather than Curie-Weiss law $1/\varepsilon=C(T-Tc)$. This temperature dependence was explained by V.V.Kirillov and V.A.Isupov based on the Gaussian distribution Eq.(5).[15] According to them, the dielectric constant are given by

$$1/(\varepsilon-\varepsilon_\infty)=1/\varepsilon_m+(T-T_0)^2/(2\varepsilon_m\sigma^2) \qquad (14)$$

Assuming $\varepsilon >> \varepsilon_\infty$, one can get

$$\sigma^2=(T-Tc)^2/2\varepsilon_m[(1/\varepsilon)-(1/\varepsilon_m)] \qquad (15)$$

Therefore the distribution F(q) is given by

$$F(\theta)=[2\pi\sigma^2]^{-1/2}\exp[-(Tc-\theta)^2/2\sigma^2) \quad (5)$$

where σ is given by

$$\sigma^2=p(1-p)/ng \quad (6)$$

Assume that the free energy of ferroelectrics is given by the following phenomenological expression:

$$G=(a/2)D^2+(c/4)D^4+(d/6)D^6 \quad (7)$$

where D is electric displacement. The phenomenological theory assumes the parameter a depends on temperature in the linear fashion;

$$a=b(T-Tc) \quad (8)$$

When the phase transition is 2nd order, c is positive. The spontaneous polarization and dielectric constant are given by (See Appendix B) ;

$$P_S^2=b(T_C-T)/c \quad (T<T_C) \quad (9)$$

$$P_S^2=0 \quad (T>T_C)$$

$$\varepsilon^{-1}=2b(T_C-T) \quad (T<T_C) \quad (10)$$

$$\varepsilon^{-1}=b(T-T_C) \quad (T>T_C)$$

When the phase transition is first order, c is negative.

3. Experimental Procedure

3.1 Powder synthesis by the molten salt method

Ceramic powders which have different compositions of PFN-PFT were prepared using a molten salt method. The procedure was as follows;

(1) Appropriate amounts of source chemicals were mixed and ground with acetone using a mortar and a pestle for about an hour to obtain uniform mixtures. Used chemicals are:

PbO (yellow powder)	J.T.Baker Chemical Co.
Fe_2O_3	Aldrich Chem. Co.
Nb_2O_5	Johnson Matthey Inc.
Ta_2O_5	Aldrich Chem. Co.
KCl	Fisher Scientific
NaCl	Johnson Matthey Inc.

The amount of PbO was 10% more than stoichiometric value. Flux/oxide ratio is 1/1. NaCl/KCl=1/1.

(2) The mixture was dried at 120°C for two hours to remove acetone.

(3) Fired in a covered alumina crucible in a box furnace at 800°C and 900°C for 1 hour.

(4) Washed in hot water to remove the chrolide.

(5) The excess PbO was removed by treating the powders with boiling acetic acid solution (5wt%) for 20 minutes.

(6) Dried at 150°C for 2 hours.

Synthesized powders were characterized by X-ray diffraction and SEM.

3.2 Sintering

Synthesized powders were mixed with 3 wt% of methocel (binder) and 0.25 wt% of Li_2CO_3 and pressed into pellets. It was reported that addition of Li_2CO_3 is effective for sintering this solid solution system.[1,2] The reason is that the oxygen vacancy created by Li^+ ions which substitute for Fe^{3+} increases the oxygen diffusion rate and enhances the grain growth. After burnig out the binder at 300°C for 2 hours, each pellet was sinterd at either 1050°C or 1100°C for 4 hours in the box furnace. The sinterd pellets were analized by X-ray diffraction. The fractured surfaces of pellets were observed using SEM.

3.3 Measurement of dielectric properties

Both sides of the sintered pellets were polished and coated with thin gold film (Thickness =1000A) by sputtering (Edwards Sputter Coater 5150B). Silver epoxy (Epoxy Technology Inc. Epo-Tek P-10) was used on the gold layer to connect cupper wire electrodes and cured at 150°C for one hour. Dielectric constant and loss tangent under weak ac fields were measured at frequencies of 1,10,100, and 1000 kHz using a Hewlett Packard 4192ALF impedance analizer with a furnace (Thernodyne type 1300) and a temperature controller (Omega CN900). The samples were first heated above Curie range and both quantities

were measured during cooling down.

DC conductivity was measured at room temperature using a HP4140B. Applied voltage was changed from 0 to 100V.

4.Results and Discussion

4.1 Characterization of powders

4.1.1 X-ray diffraction

Synthesis conditions and chemical compositions of powders and the phases of powders determined by X-ray diffraction are shown in Table 2. X-ray diffraction patterns of PFT synthesized at 800°C and 900°C are attached in Appendix A. At reaction temperature 800°C, the samples which had more Ta consisted of several phases. The amount of the second phase decreased as the concentration of Nb increased. Although the tolerance factor and the electronegativity difference of PFN and PFT are almost same, this result indicates that PFT is more difficult to form than PFN.

The main component of the second phase was $Pb_3Ta_2O_8$. Thus the formation reactions of PFT is considered as follows;

$$3PbO+Ta_2O_5 \rightarrow Pb_3Ta_2O_8$$

$$Pb_3Ta_2O_8+PbO+Fe_2O_3 \rightarrow Pb_4Ta_2Fe_2O_{12}$$

In the synthesis of PFN, the second phase was $Pb_3Nb_4O_{13}$.[2] But no peak of $Pb_3Ta_4O_{13}$ was observed in this study.

Lattice constants of each compositions were calculated assuming all the crystal systems are cubic. The results are shown in Table 2. The lattice constant

Table.2 Synthesized powders

No.	Composition	reaction temp.(°C)	Phase	Lattice Constant(A)	Particle size(μm)
1	PFN	850(2h)	P	4.007	
2	0.8PFN+0.2PFT	800	P	4.003	1.0
3	0.6PFN+0.4PFT	800	P	3.997	
4A	0.4PFN+0.6PFT	800	P		0.5
4B	0.4PFN+0.6PFT	900	P	4.003	
5A	0.2PFN+0.8PFT	800	P+P3T2		
5B	0.2PFN+0.8PFT	900	P	4.000	
6A	PFT	800	P+P3T2+others		0.3
6B	PFT	900	P	3.997	0.5

P;Perovskite P3T2;$Pb_3Ta_2O_8$

*Sample 1 was synthesized by Mr.Chiu.

increased slightly from PFT to PFN. This result agrees with the reported lattice constants (PFN:4.013A, PFT:4.011A) of each crystals.

No superlattice peaks were observed for the studied solid solutions. B-site cations seem to be completely disordered.

4.1.2 SEM

Scanning electron micrographs (SEM) of synthesized powders (Sample 2,4,6A, and 6B) are shown in Fig.1. The average particle size is shown in Table 2. The particle size distribution was very large for all the powders. As Nb content increased in the composition, the average particle size increased. It is reasonable because formation rate of PFN is faster than that of PFT. In sample 6A (PFN synthesized at 800°C), there were two kinds of particles: small particles and large flat plates. It is likely that the small particles are perovskite and large flat plates are the second phase, but it was not confirmed.

4.2 Characterization of sintered pellets

4.2.1 X-ray diffraction

Phases of sintered pellets determined by X-ray diffraction are shown in Table 3. X-ray diffraction patterns of PFT are attached in Appendix A. Samples 5A(0.8PFT +0.2PFN) and 6A(PFT), which had second phases as powders, converted to pure perovskite after sintering.

On the other hand, samples synthesized at 900°C decomposed into perovskite and P3T2 especially at higher sintering temperature. A severe contrast can be seen in the sample 6B(PFT); one sintered at 1050°C consists of pure perovskite, however the other sintered at 1100°C is P3T2. This result implies that PFT is rather unstable compared to PFN. The cause of this decomposition is probably the evaporation of lead during sintering.

4.2.2 SEM

SEMs of fractured surfaces of sintered pellets (Sample 2,4,6A, and 6B) are shown in Fig.2-5. The average particle sizes are shown in Table 4. Comparing the samples synthesized at 800°C (Samples 2,4, and 6), we could observe that the grain size increased as the ratio of Nb increased. The grain size increased as the particle size increased. The grain size also increased with the sintering temperature. In these samples, there are clusters of small grains distributed among larger grains. In other words, the grain size distribution is not uni-modal, but bi-modal.

The behavior of the samples synthesized at 900°C (Sample 6B) is quite different from those synthesized at 800°C. The grain sizes are much larger, and the sintering is much more advanced especially at 1100°C. The decomposition into P3T2 also occured between the sample sintered at 1050°C and the sample sintered at 1100°C. This result indicates that the mobility of ions are much higher in these samples. This high mobility

Table 3 Sintered Pellets

Sample No.		Sintering temperature 1050°C	1100 °C
1	PFN	P	P
2	0.8PFN+0.2PFT	P	P
3	0.6PFN+0.4PFT	P	P
4A	0.4PFN+0.6PFT	P	P
4B		P+P3T2	P+P3T2
5A	0.2PFN+0.8PFT	P	P
5B		P	P+P3T2
6A	PFT	P	P
6B		P	P3T2

P;Perovskite P3T2;$Pb_3Ta_2O_8$

Table 4 Grain size

Sample		Temp.(°C)	1050°C	1100°C
2	0.8PFN+0.2PFT	800	10 (μm)	12 (μm)
4A	0.6PFN+0.4PFT	800	8	
6A	PFT	800	3	8
6B	PFT	900	20	

enhanced evaporation of lead and caused the decomposition. Thus the defect structures of powders synthesized at 800°C and those at 900°C must be quite different, but we could not identify it only from this information.

4.3 Dielectric Properties

4.3.1 Temperature dependence of dielectric constant

Fig.6-17 show the temperature dependence of dielectric constant and tangent loss at various frequencies. As the composition changes from PFN to PFT, the Curie temperature decreased. Since we could not cool samples below room temperature, we could measure the Curie range only of sample 1(PFN) and 2(0.8PFN+0.2PFT). In this result, the following characteristics were observed;

(1) Dielectric constant was higher at low frequency especially in high temperature. It was always accompanied by high tangent loss.

(2) Generally, samples sintered at 1050°C had lower frequency dependence than those sintered at 1100°C.

(3) There was no peak or large change of tangent loss around the Curie temperature.

(4) The maximum point of dielectric constant did not depend on frequency.

As mentioned in 2.2, the Curie temperature of the typical relaxor depends on frequency and the tangent loss

has maximum at the different temperature from the Curie temperature. However these characteristics were not observed in the PFN-PFT system, even though the PFN-PFT system showed a broad dielectric phase transition.

High dielectric constant and tangent loss in low frequency range can be explained by ion migration. At low frequency, ions can jump from place to place. It causes additional polarization, and its relaxation increases tangent loss. The difference between the samples at 1050°C and 1100°C comes from the different micro-structures of each samples.

4.3.2 DC conductivity

DC conductivity at various electric fields is shown in Fig.18-19. Among samples synthesized at 800°C, those sintered at 1050°C have a tendency that pure PFN or PFT has lower conductivity than solid solution but those sintered at 1100°C do not have such a tendency.

No relation between tangent loss and DC conductivity was observed.

4.3.3 Calculation of compositional fluctuation

To calculate compositional fluctuation, we need to estimate Curie temperatures of each samples. It was assumed that pure PFT has a Curie point at -40°C as Ref[1]. Using this point and measured Curie temperatures

of sample 1 and 2, Curie temperatures of other compositions were estimated as in Fig.20. There was a slight difference of Curie temperature due to the sintering temperature. Obtained values of Curie temperaure are shown in Table 5.

Using those Curie temperatures, $1/\varepsilon$ vs. $(T-Tc)^2$ was plotted in Fig.21. Dielectric constants at 1MHz were used for this plotting because there is less effect of space charge in this frequency range. Very good linear relation can be seen in sample 1(PFN) and 2(0.8PFN+0.2PFT). But in the other samples, the relation is uncertain because we do not have dielectric constant around Curie temperature of these samples. Using Eq.(15), σ was obtained from these figures. The obtained value of σ for each samples are shown in Table 6.

If we consider compositional fluctuation of only Nb and Ta, the distribution of composition is described by probability Eq.(2). The standard diviation of such a distribution is given by

$$\sigma = (np(1-p))^{1/2} \qquad (16)$$

Thus if Nb and Ta are distributed randomly, σ is maximum at the composition 0.5PFN+0.5PFT. In sample 1,2, and 3, where we could get more reliable data, σ is changing in this manner.

Assuming that each Kanzig region undergoes a first-

Table 5 Curie Temperature

Sample No.		Curie Temp.(°C) 1050°C	1100°C
1	PFN	92	88
2	0.8PFN+0.2PFT	55	45
3	0.6PFN+0.4PFT	26	17
4A	0.4PFN+0.6PFT	0	-5
5A	0.2PFN+0.8PFT	-20	-23
6A	PFT	-40	-40

order ferroelectric phase transition, temperature dependence of dielectric constants were calculated for sample 1,2 and 3. The detail of this calculation is in Appendix C. The results are shown in Fig.22. Solid lines are calculated results for each samples. Table 6 shows the used value for each parameter. The value of Curie constant b is reasonable compared to those of other perovskite oxides.[16] The value of σ in this calculation is smaller than that from Eq.(15). The reason for this discrepancy is that only the Kanzig region which has Curie temperature close to the measured temperature is considered and temperature dependence of ε_m is neglected to derive Eq.(15). The calculated results gave higher dielectric constant in high temperature region. It might be because Eq.(12) overestimates the dielectric constant of paraelectric region compared to that of ferroelectric region. Similar calculation was performed by J.Kuwata et al for PZN.[17]

Even though there was some descrepancy between the experimental data and the calculated result, the ferroelectric behavior of the PFN-PFT was well described by the compositional fluctuation model.

Table 6 Obtained Parameters

No.	Sintering Temp. (°C)	σ [1] (K)	σ [2] (K)	b ($10^{-6}K^{-1}$)	T_c-T_Q
1	1050	29	25	2.2	6
	1100	30	25	2.6	6
2	1050	40	30	3.4	6
	1100	37	32	2.8	6
3	1050	54	40	2.5	6
	1100	59	33	2.2	6
4A	1050	65			
	1100	52			
5A	1050	54			
	1100	73			
6A	1050	83			
	1100	81			

1) Obtained from Eq.(15).

2) Obtained to fit calculated curves.

5. Summary

Various compositions of PFN-PFT solid solution were synthesized by the molten salt method at 800°C and 900°C. Higher temperature was necessary to form pure perovskite of PFT than PFN. However those sinthesized at higher temperature tended to decompose during sintering. The particle size was not uniform and increased from PFT to PFN.

The distribution of grain size in the sintered pellets was bi-modal. The grain size increased as the particle size increased. Those synthesized at 900°C had quite a different behavior from those synthesized at 800°C during sintering.

Each composition of PFN-PFT system showed a broad dielectric phase transition in the different temperature range. This behavior was well described by the statistical model of compositional fluctuation.

Reference

1. M.Halmi, G.Desgardin, and B.Raveau, "Low-Temperatures Sintered Lead Tantalate Based Ceramics of High Dielectric Constants", Mater.Lett., 5[3], 103-110(1987)

2. C.Chiu,"Low Temperature Synthesis and Properties of lead ferroniobate $Pb(Fe_{0.5}Nb_{0.5})O_3$", M.S.Thesis, VPI&SU 1990

3. S.S.Lopatin, T.G.Lupeiko, and I.I.Ivleva, "The preparation of Lead Ferroniobate in the Presence of Molten Sodium and Potassium Chloride" ,Zh.Neorg.Khim. (Russ.J.of Inorganic Chem.), 32[4],865-868(1987)

4. Y.Hayashi, T.Kimura, and T.Yamaguchi, "Preparation of Acicular NiZn-Ferrite Powders", J.of Mater.Sci., 21,2876-2880(1986)

5. Y.Hayashi, T.Kimura, and T.Yamaguchi, "Preparation of Rod-shaped $BaTiO_3$ Powders", J.of Mater.Sci., 21,757-762(1986)

6. T.Kimura and T.Yamaguchi, "Morphology of Bi_2WO_6 Powders Obtained in the Presence of Fused Salts", J.of Mater.Sci., 17,1863-1870(1982)

7. W.Brixel, R.Boutellier, and H.Schmid, "Flux Growth and Characterization of Single Crystals of the Perovskites Pb_2FeTaO_4 and Pb_2CsWO_6", J.of Crystal Growth, 82,396-404(1987)

8. S.A.Mabud, "X-ray and Newtron Diffraction Studies of Lead Iron Niobate Ceramics and Single Crystals", Phase Transitions, 4, 183-200(1984)

9. F.S.Galasso, "Structures, Properties, and Preparation of Perovskite-Type Compounds", Pergamon

Press,1969

10. L.Pauling, "The Nature of Chemical Bonds", Cornell University, New York, 1960

11. G.A.Smolenski, Proc.2nd Meet. Ferroelectricity, Kyoto, 1969, J.of Phys.Soc.Jpn. 28(1970) Suppl. p.26

12. C.A.Randall and A.S.Bhalla, "Nonostructual-Property Relation in Complex Lead Perovskites", Jpn.J.Appl.Phy., 29[2],327-333(1990)

13. I.H.Burnskill, H.Schmid, and P.Tissot, "The Characterization of High Temperature Solution-Grown Single Crystals of $Pb(Fe_{0.5}Nb_{0.5})O_3$", Ferroelectrics,37, 547-550(1981)

14. B.N.Rolov, "Effect of Composition Fluctuation on Unsharp Ferroelectric Transition", Soviet Physics Solid State 6[7], 1676-1678(1965)

15. V.V,Kirillov and V.A.Isupov, "Relaxation Polarization of $PbMg_{1/3}Nb_{2/3}O_3$(PMN)-A Ferroelectric with a Diffused Phase Transition", Ferroelectrics, 5, 3-9(1973)

16. C.Kittel, "Introduction to Solid State Physics", John Wiley & Sons, New York 1976

17. J.Kuwata, K.Uchino, and S.Nomura, "Diffuse Phase Transition in Lead Zinc Niobate", Ferroelectrics,22, 863-867(1979)

Appendix A X-ray diffraction

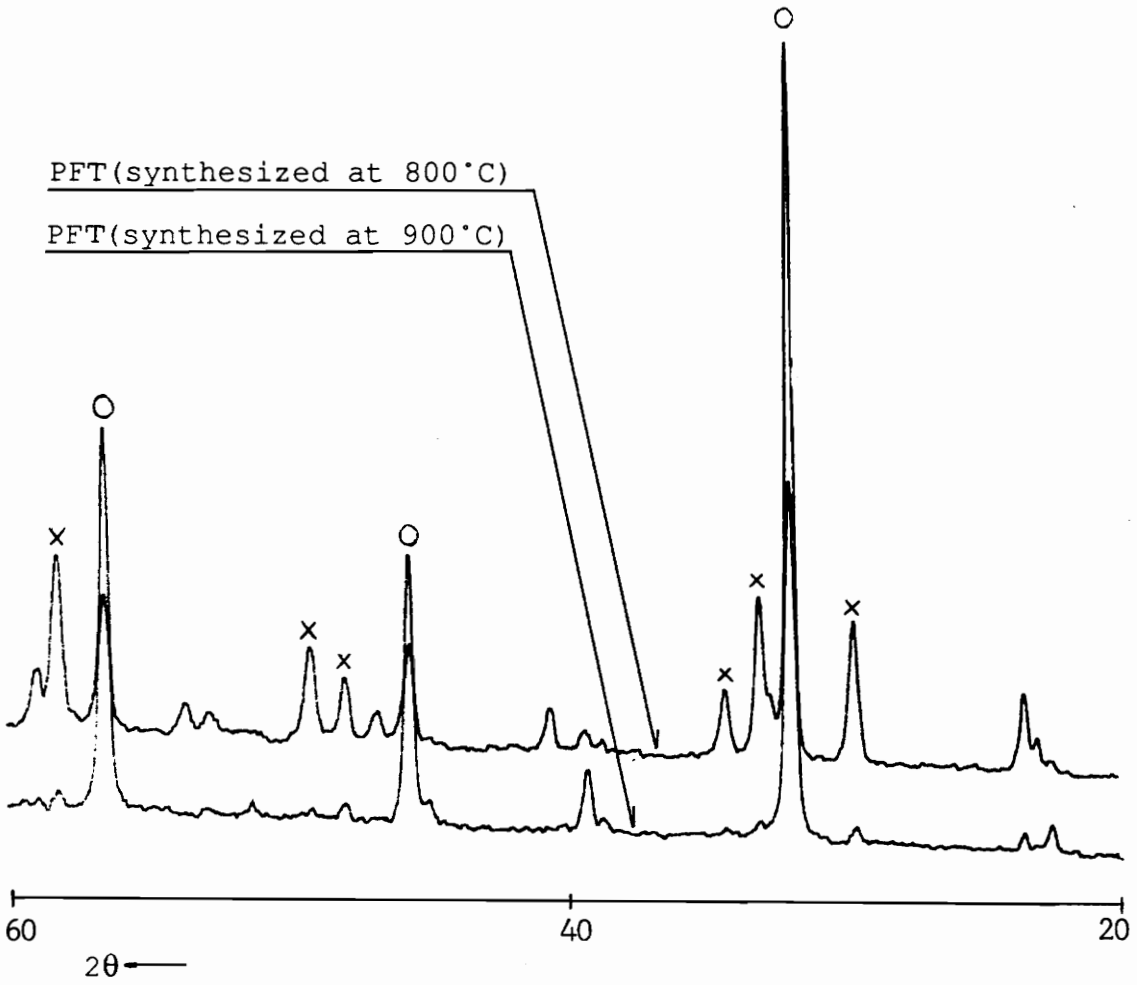

○ : peaks of perovskite
× : peaks of P3T2

Fig.A-1 X-ray diffraction of powder samples.
(CuKα: λ=1.5418 A)

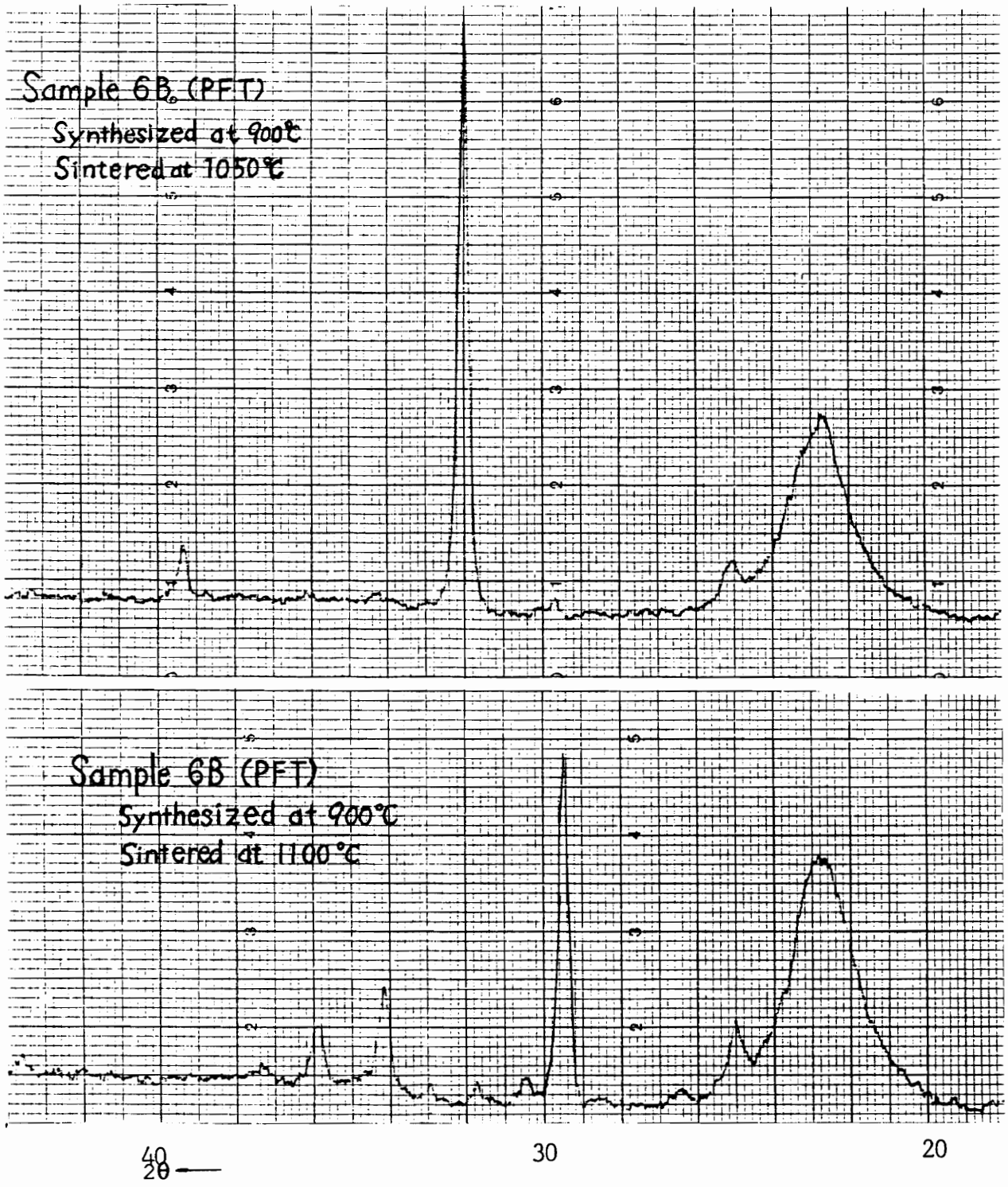

Fig.A-2 X-ray diffraction of sintered pellets.
(CuKα: λ=1.5418A)

32-522

d	2.84	1.64	2.01	4.02	$Pb(Fe_{0.5}Nb_{0.5})O_3$
I/I_1	100	55	40	16	Lead Iron Niobium Oxide

Rad. CuKα λ 1.54188 Filter Mono. Dia.
Cut off I/I_1 Diffractometer I/I cor. 9.13
Ref. Pfoertsch and Ruud, Penn State University (1981)

Sys. Cubic S.G. $Pm\bar{3}m$ (221)
a_0 4.0148(1) b_0 c_0 A C
α β γ Z 1 Dx 8.456
Ref. Ibid.

εα nωβ εγ Sign
2V D mp Color Rust
Ref. Ibid.

Specimen provided by J. Canner, Erie Technological Products, State College, Pennsylvania.
Perovskite Structure Type.
F_{18} = 80.14(0.0125,18).
Si (SRM-640) used as internal standar (a_0=5.43088Å).

d A	I/I_1	hkl		I/I_1	
4.015	16	100			
2.838	100	110			
2.318	25	111			
2.008	40	200			
1.796	9	210			
1.639	55	211			
1.420	25	220			
1.3385	3	221			
1.2699	18	310			
1.2107	3	311			
1.1590	6	222			
1.1135	1	320			
1.0731	18	321			
1.0040	2	400			
0.9737	1	410			
.9464	7	330			
.9210	1	331			
.8978	5	420			

15-416

d	2.84	1.64	2.00	4.02	$Pb_4Fe_2Ta_2O_{12}$ $4PbO.Fe_2O_3Ta_2O_5$
I/I_1	100	30	25	10	Lead Iron Tantalum Oxide

Rad. CuK λ 1.5418 Filter Ni Dia.
Cut off I/I_1 Diffractometer
Ref. Argyle & Hummel, J. Am. Ceram. Soc. 46 (1963)

Sys. S.G.
a_0 b_0 c_0 A C
α β γ Z Dx
Ref.

εα nωβ εγ Sign
2V D mp Color
Ref.

d Å	I/I_1	hkl		I/I_1	hkl
4.02	10				
3.05	10				
2.84	100				
2.64	4				
2.32	10				
2.00	25				
1.863	4				
1.637	30				
1.590	4				
1.526	2				
1.417	12				
1.268	10				
1.158	2				

ASTM cards of PFN and PFT

Appendix B The phenomenological theory of ferroelectric phase transition

In the phenomenological theory, the free energy of the ferroelectric is expressed in the simple polynominal form

$$G=(a/2)D^2+(c/4)D^4+(d/6)D^6 \qquad (B-1)$$

where energy is measured from the non-polar phase and D is electric displacement. First- and second-order phase transitions can be discribed assuming c and d are independent of temperature. With this assumption, the order of transition depends on the sign of c. (d must be positive so that the system is stable when $D\rightarrow\infty$.)

B-1. Second-order ferroelectric phase transitions

When c is positive, Eq.(B-1) can describe second-order phase transitions. In this case, the term D^6 can be neglected because it does not give any additional information. When parameter a is positive, the free energy curve has a single minimum at D=0, but when a is negative, the curve acquires a double-minimum form with minimum at non-zero values of displacement. Since $E=(\partial G/\partial D)_T$, the minima describes the equilibrium value of zero-field displacement (i.e. spontaneous polarization Ps) as a function of temperature. It is clear that Ps undergoes a continuous (second-order) phase transition as a passes through zero. Thus it is asssumed that near the Curie point Tc, the parameter a depends on temperature in the linear fashion;

$$a=b(T-Tc) \qquad (B-2)$$

On the other hand, defferentiating the free energy respect to D gives

$$E=aD+cD^3+dD^5 \qquad \text{(B-3)}$$

and the inverse isothermal permitivity is given by

$$\kappa=dE/dD \qquad \text{(B-4)}$$

Therefore a is in fact the reciprocal permitivity at zero field in non-polar phase;

$$\kappa=a=b(T-Tc) \qquad (T>Tc) \qquad \text{(B-5)}$$

Following Eq.(B-3), the spontaneous polarization below Tc is given by

$$Ps^2=b(T-Tc)/c \qquad \text{(B-6)}$$

From Eq.(B-3) and Eq.(B-4),

$$\kappa=b(T-Tc)+3cPs^2 \qquad \text{(B-7)}$$

Substituting Eq.(B-6) into Eq.(B-7) gives

$$\kappa=2b(Tc-T) \qquad (T<Tc) \qquad \text{(B-8)}$$

B-2. First-order ferroelectric phase transitions

When c is negative, the term D^6 cannot be neglected. Again a is assumed to have a form

$$a=b(T-To) \qquad (B-9)$$

but where To is called the paraelectric Curie temperature and is not equal to the transition temperature Tc. Conditions for a zero-field first-order transition is that both G and its first derivative respect to D are zero; that is when

$$(b/2)(T-To)+(c/4)Ps^2+(d/6)Ps^4=0 \qquad (B-10)$$

$$b(T-To)+cPs^2+dPs^4=0 \qquad (B-11)$$

are simultaneously satisfied. The solution is

$$T=Tc=To+(3/16)c^2/(bd) \qquad (B-12)$$

Zero-field permitivity can be deduced from Eq.(B-3) as

$$\kappa=b(T-To)+3cPs^2+5dPs^4 \qquad (B-13)$$

When T<Tc, solving Eq.(B-11) and Eq.(B-13) gives

$$\kappa=(c^2/d)(1+(1-4bd)(T-To)/c^2)^{1/2})-4b(T-To) \qquad (B-14)$$

Appendix C Calculation of dielectric constant

When the distribution of Curie temperature of each Kanzig region is given by Gaussian function, the total dielectric constant at temperature T is given by

$$\kappa(T)=(2\pi\sigma^2)^{-1/2}\int_0^{\infty}\kappa(T,\theta)\exp[-(Tc-\theta)^2/2\sigma^2]d\theta \quad (C-1)$$

where $\kappa(T,\theta)$ is recoprocal dielectric constant of Kanzig region which has Curie temperature at θ. Substituting Eq.(12) into Eq.(C-1) gives

$$\kappa(T)=\frac{b}{\sqrt{2\pi\sigma^2}}\left[\int_0^{T}(\theta-Tc-\Delta)\exp[-(\theta-Tc)^2/2\sigma^2]d\theta + \int_T^{\infty}\frac{16\Delta}{3}\left(1+\sqrt{1-\frac{3(\theta-Tc-\Delta)}{4\Delta}}\right)\exp\left[\frac{(\theta-Tc)^2}{2\sigma^2}\right]d\theta\right] \quad (C-2)$$

where

$$\Delta=Tc-To=(3/16)c^2/(bd) \quad (C-3)$$

We used "matematica" to calculate this integration. The integration range was 0K to 1000K. If unnecessary large range were used, the calculation would give a wrong result.

The parameters which have to be determined are as follows;

Tc: Average Curie temperature

σ : Broadness of Curie temperature distribution

b : Curie constant

Δ : Difference between Curie temperature and paraelectric Curie temperature

Δ was fixed as 6 for all the calculation. All the other parameters were determined to fit the calculated curve to the experimental data by try and error.

(A)
0.8PFN
+
0.2PFT
(800°C)

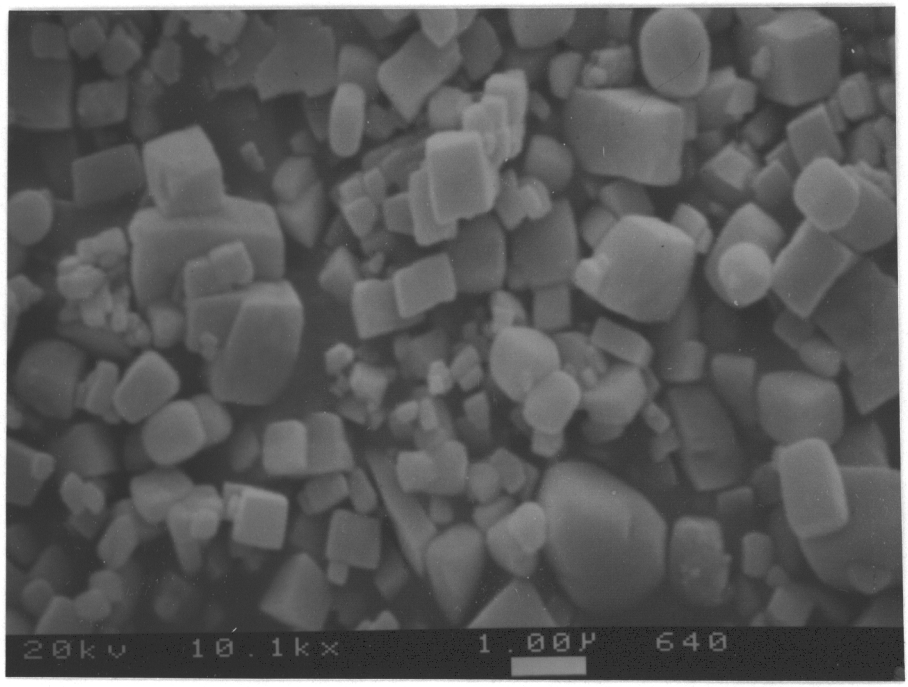

(B)
0.6PFN
+
0.4PFT
(800°C)

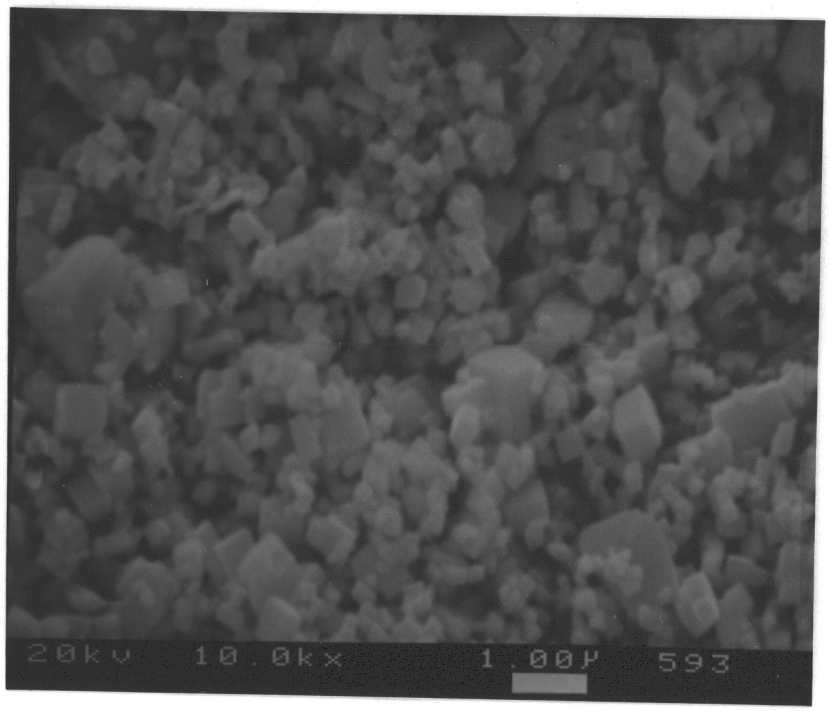

Fig.1 SEM of (A) Sample 2 (B) Sample 4A (C),(D) Sample 6A (E) Sample 6B

(C)
PFT
(800°C)

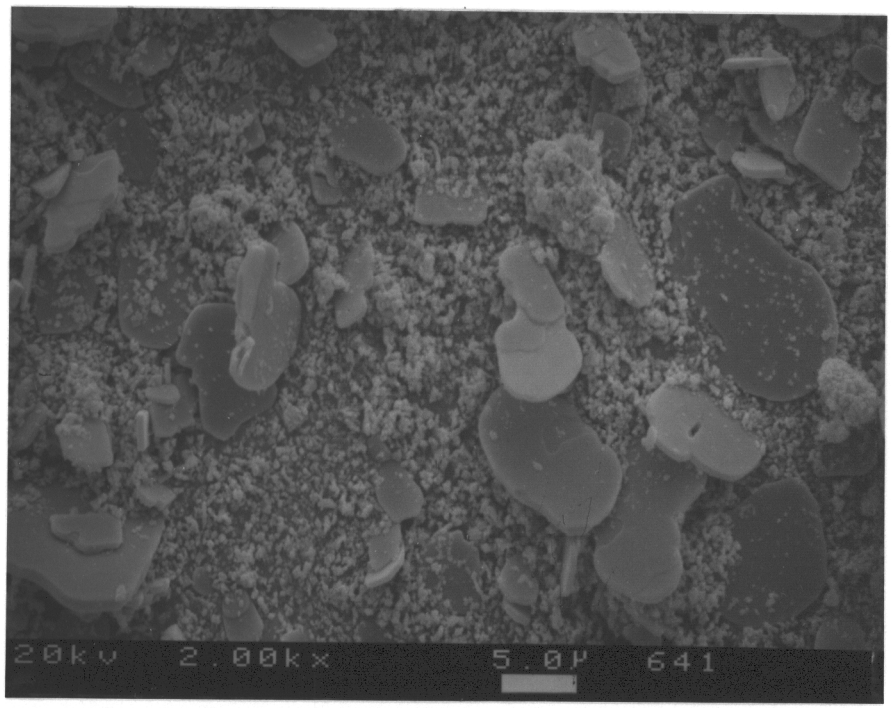

(D)
PFT
(800°C)

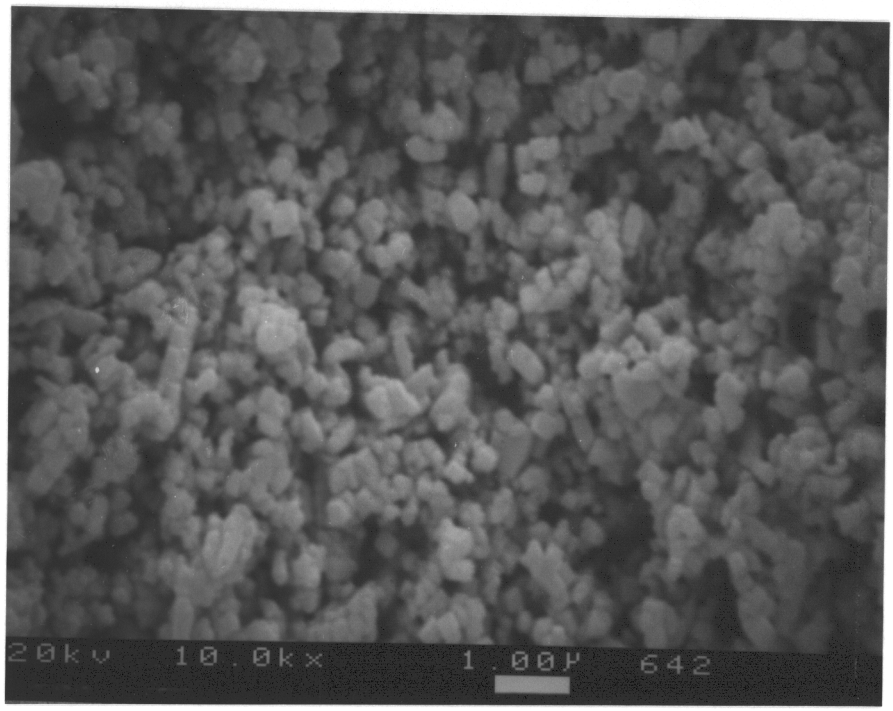

Fig.1 Continued.

(E)
PFT
(900°C)

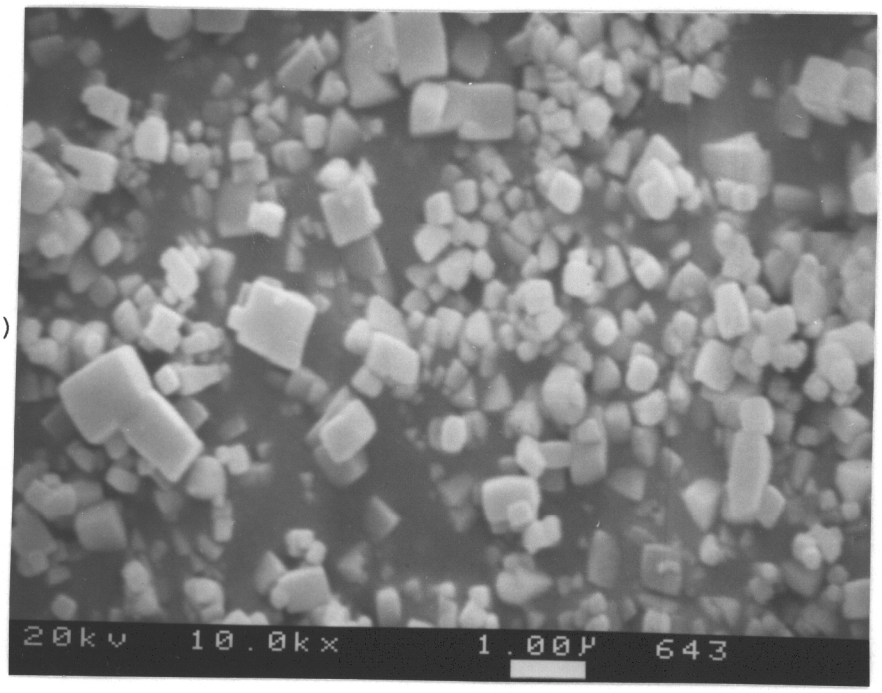

Fig.1 Continued

(A)

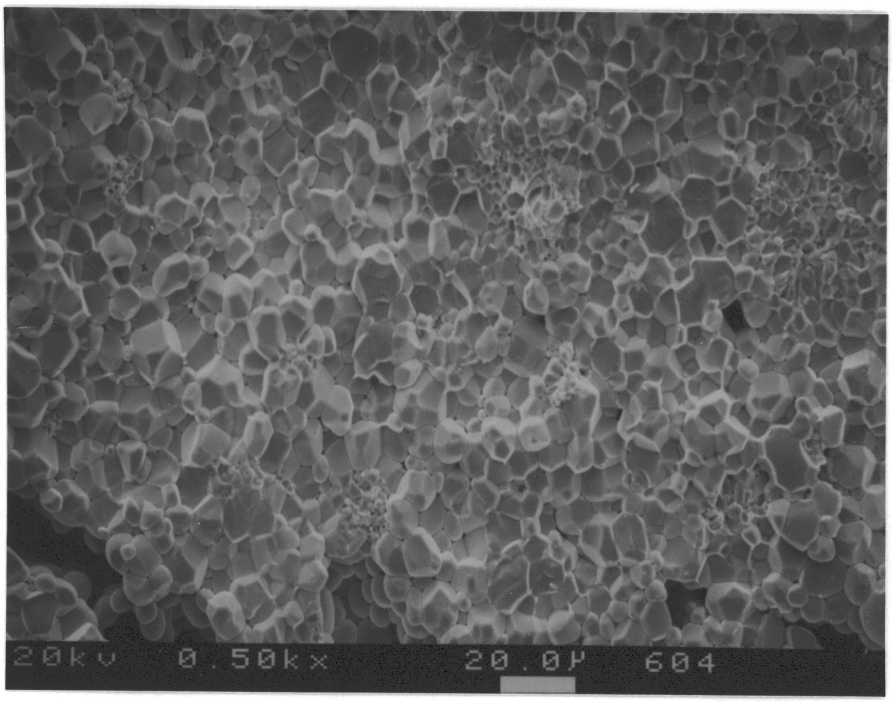

(B)

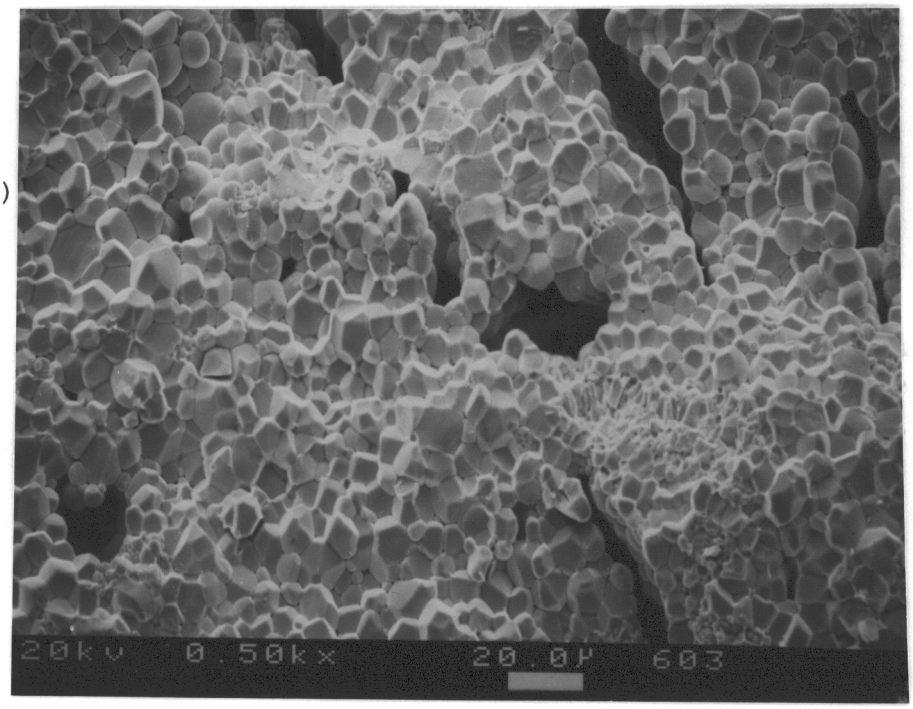

Fig.2 SEM of Sample 2 (0.8PFN+0.2PFT) (A) Sintered at 1050°C, (B) at 1100°C.

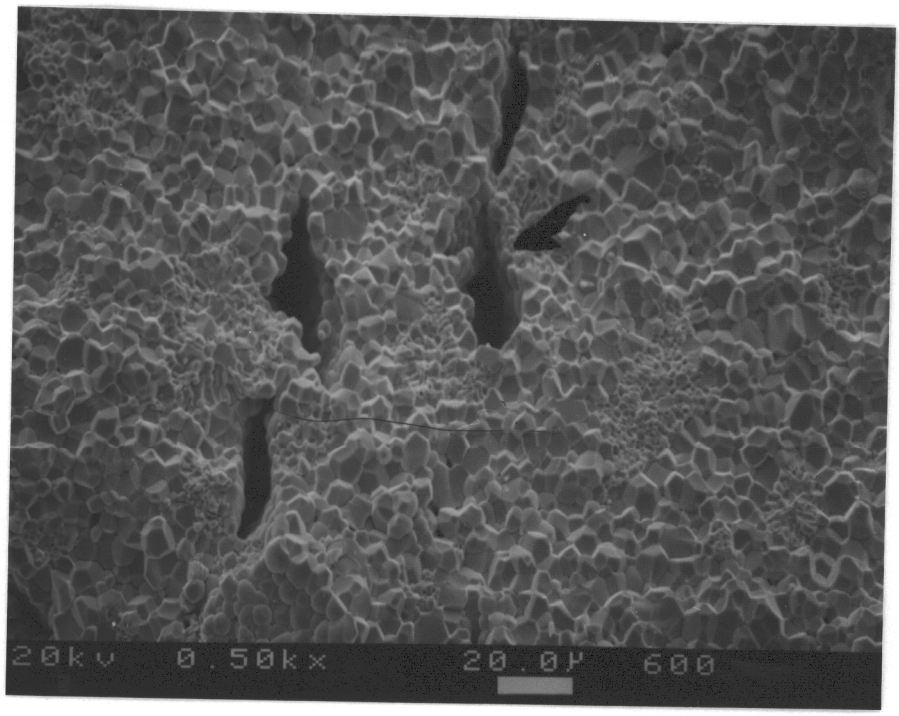

Fig.3 SEM of Sample 4A (0.6PFN+0.4PFT synthesized at 800°C, sintered at 1050°C)

(A)

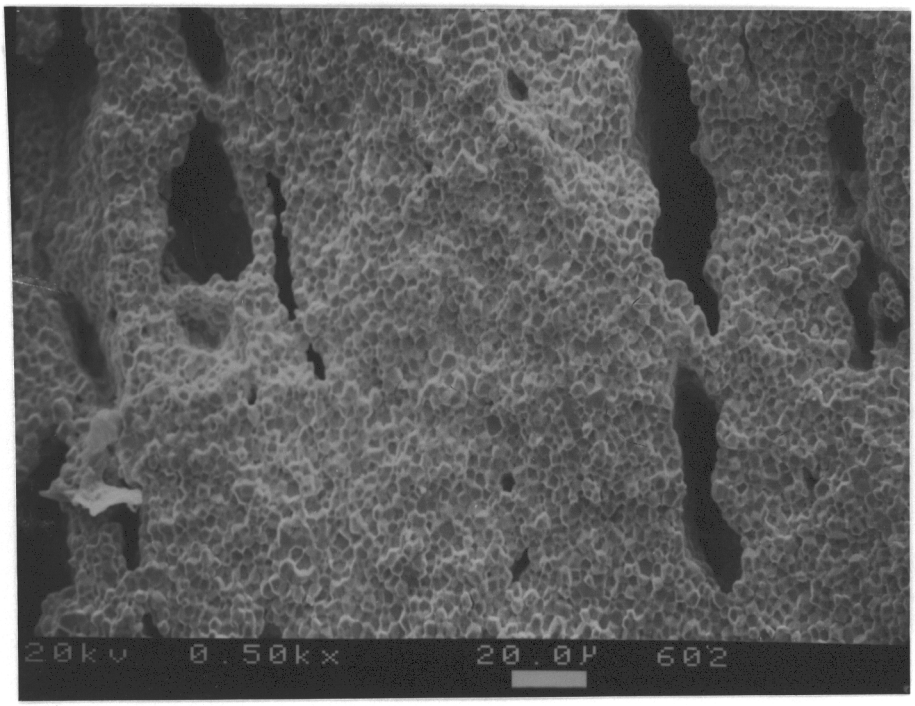

(B)

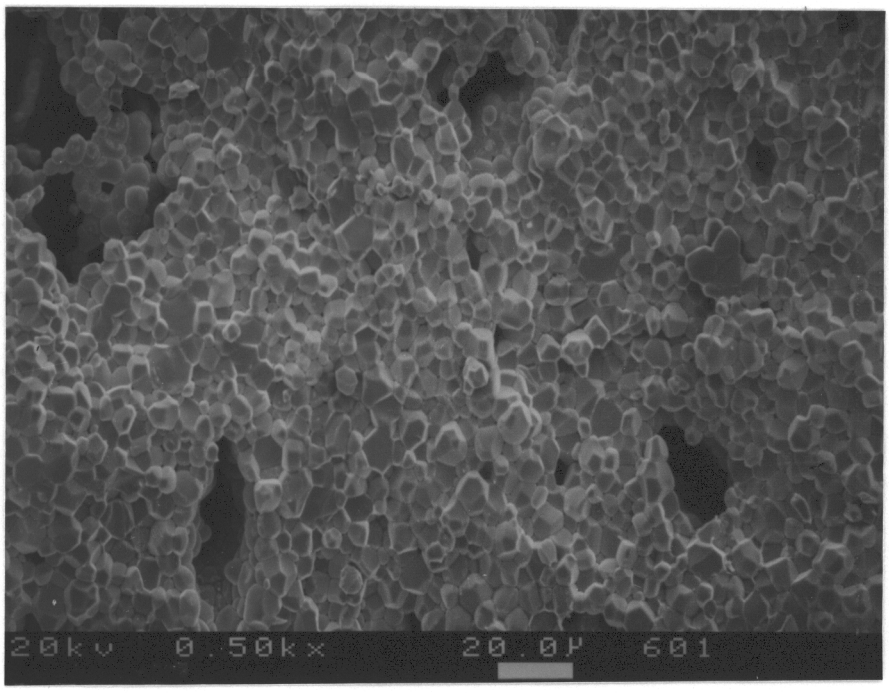

Fig.4 SEM of Sample 6A (PFT synthesized at 800°C) (A) sintered at 1050°C, (B) at 1100°C.

(A)

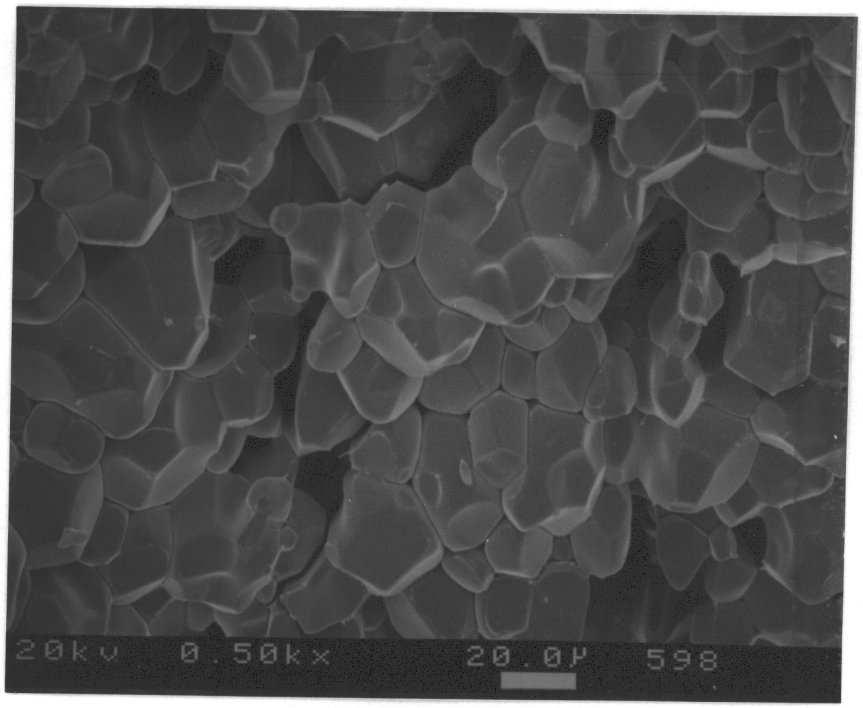

(B)

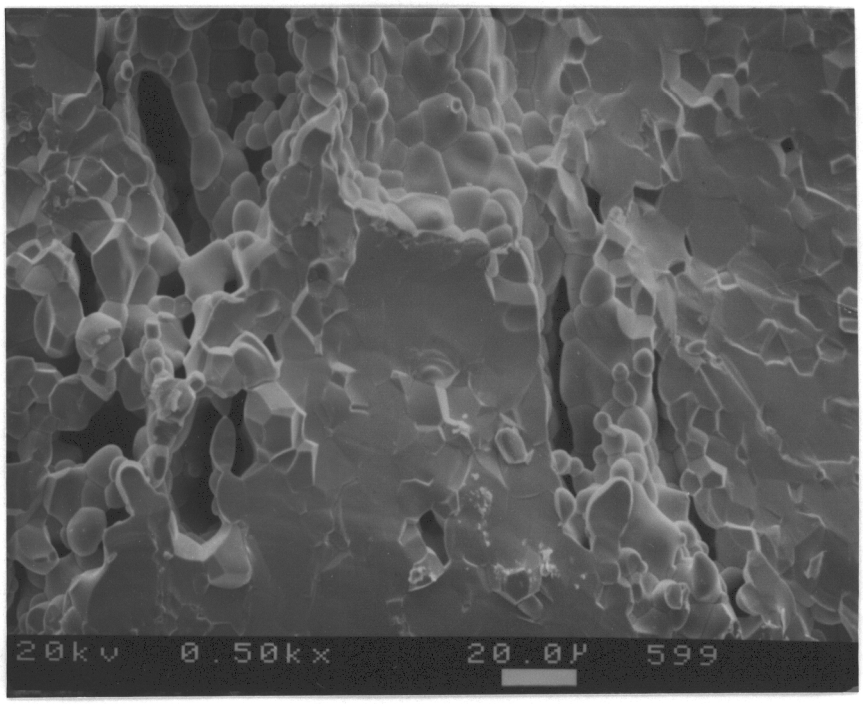

Fig.5 SEM of Sample 6B (PFT synthesized at 900°C) (A) sintered at 1050°C, (B) sintered at 1100°C.

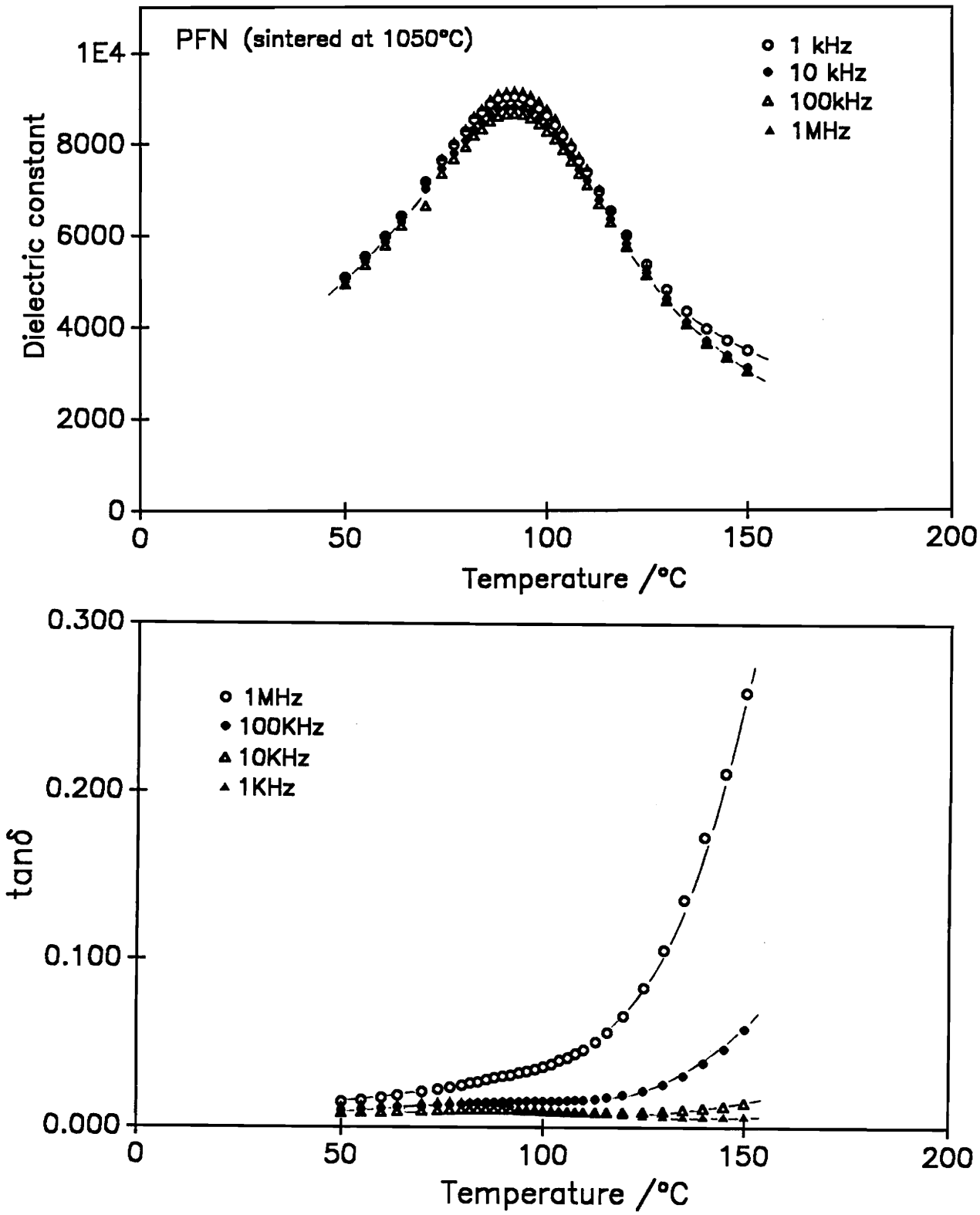

Fig.6 Dielectric property of sample 1 (PFN synthesized at 850°C)sintered at 1050°C.

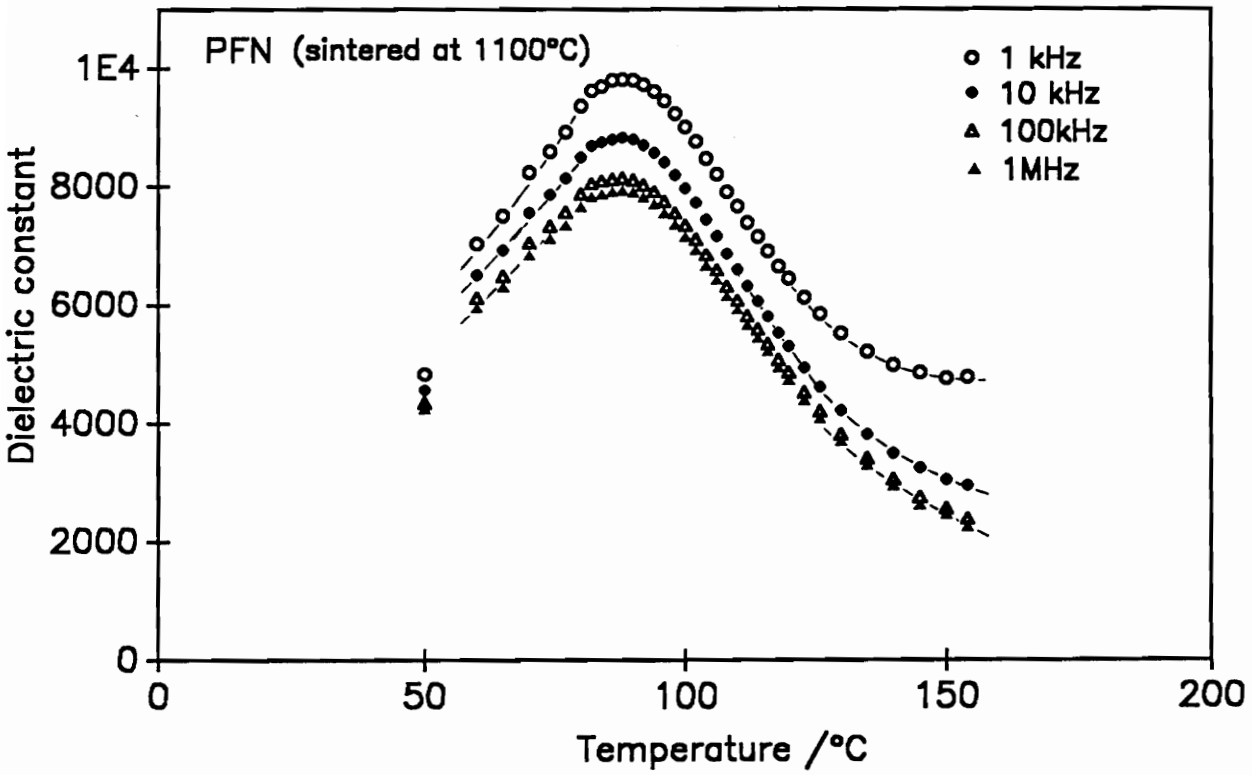

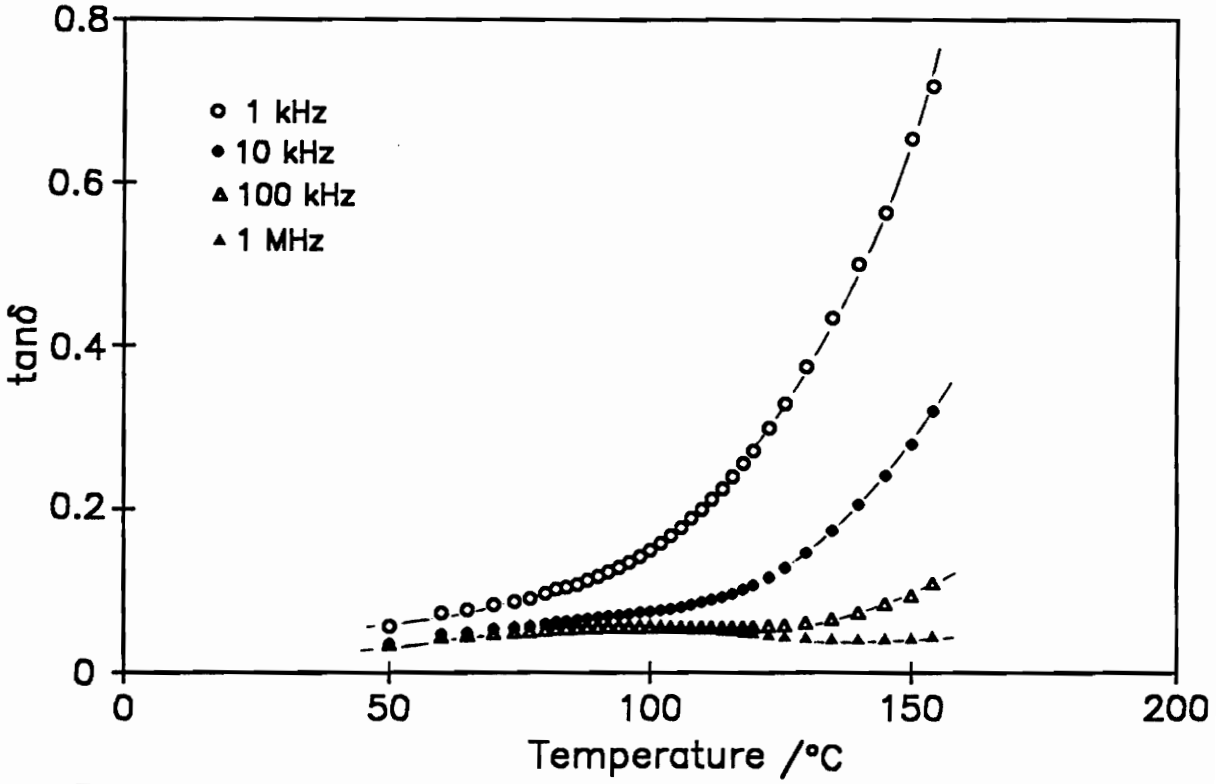

Fig.7 Dielectric property of sample 1 (PFN synthesized at 850°C) sintered at 1100°C.

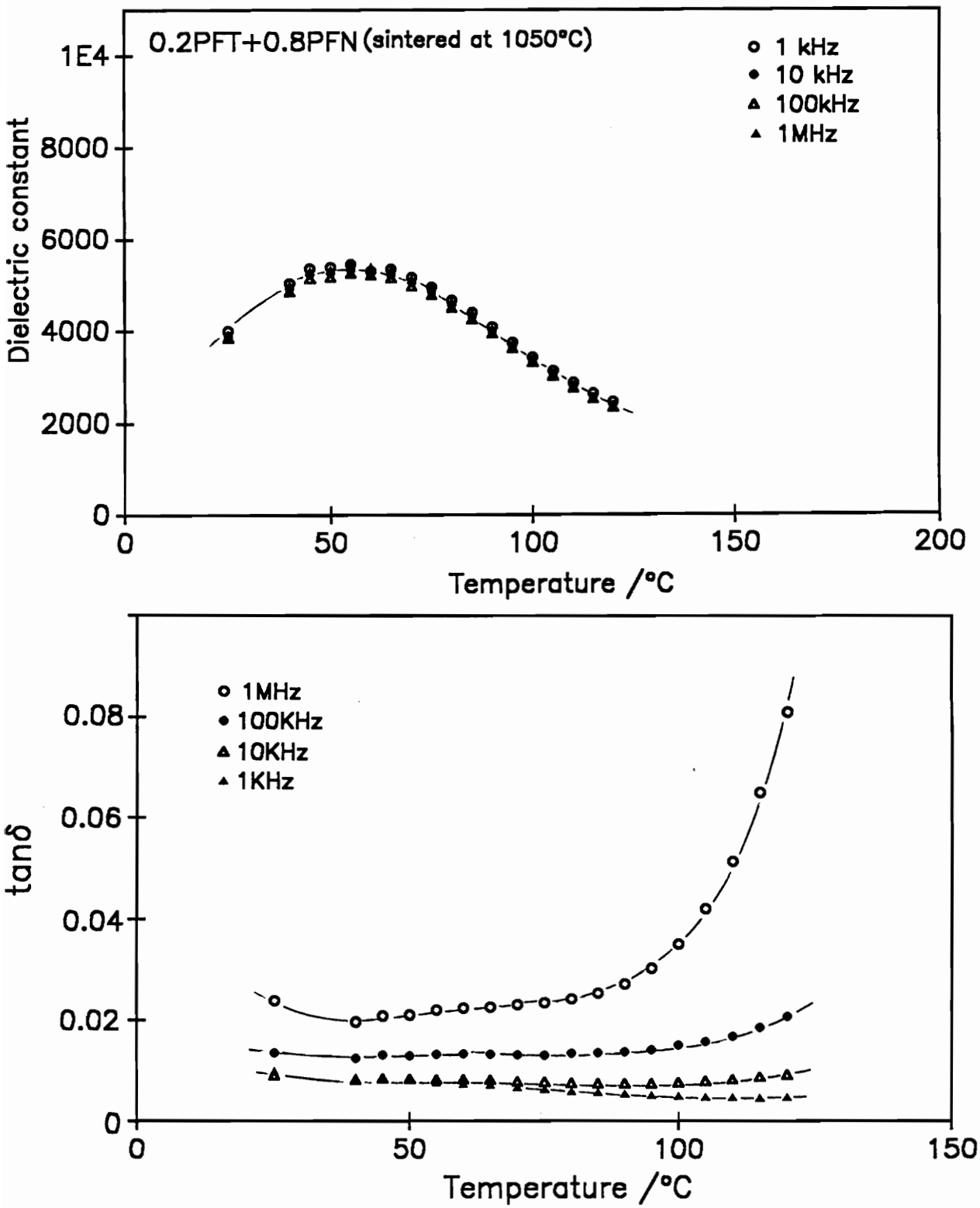

Fig.8 Dielectric property of sample 2 (0.8PFN+0.2PFT synthesized at 800°C) sintered at 1050°C.

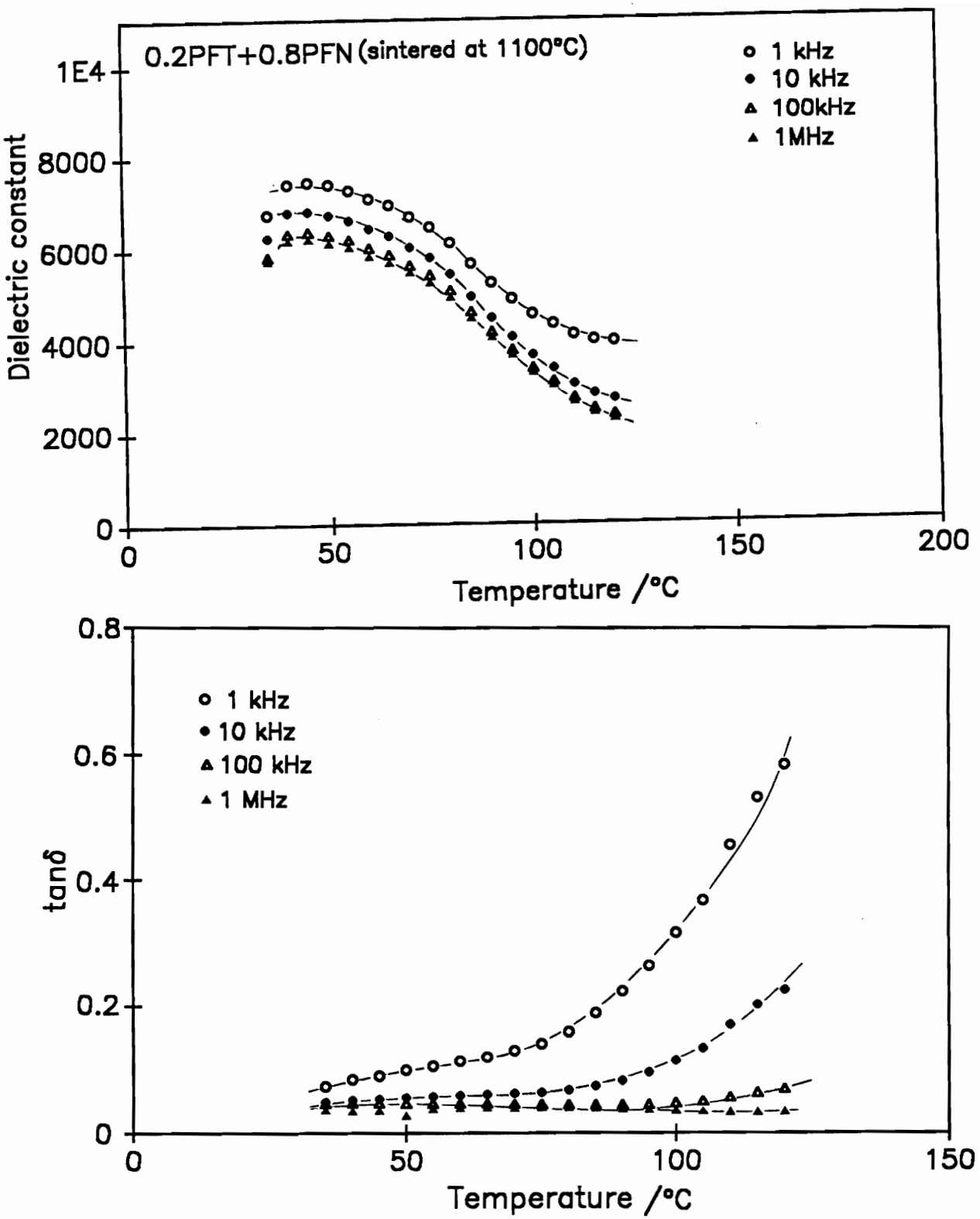

Fig.9 Dielectric property of sample 2 (0.8PFN+0.2PFT synthesized at 800°C) sintered at 1100°C.

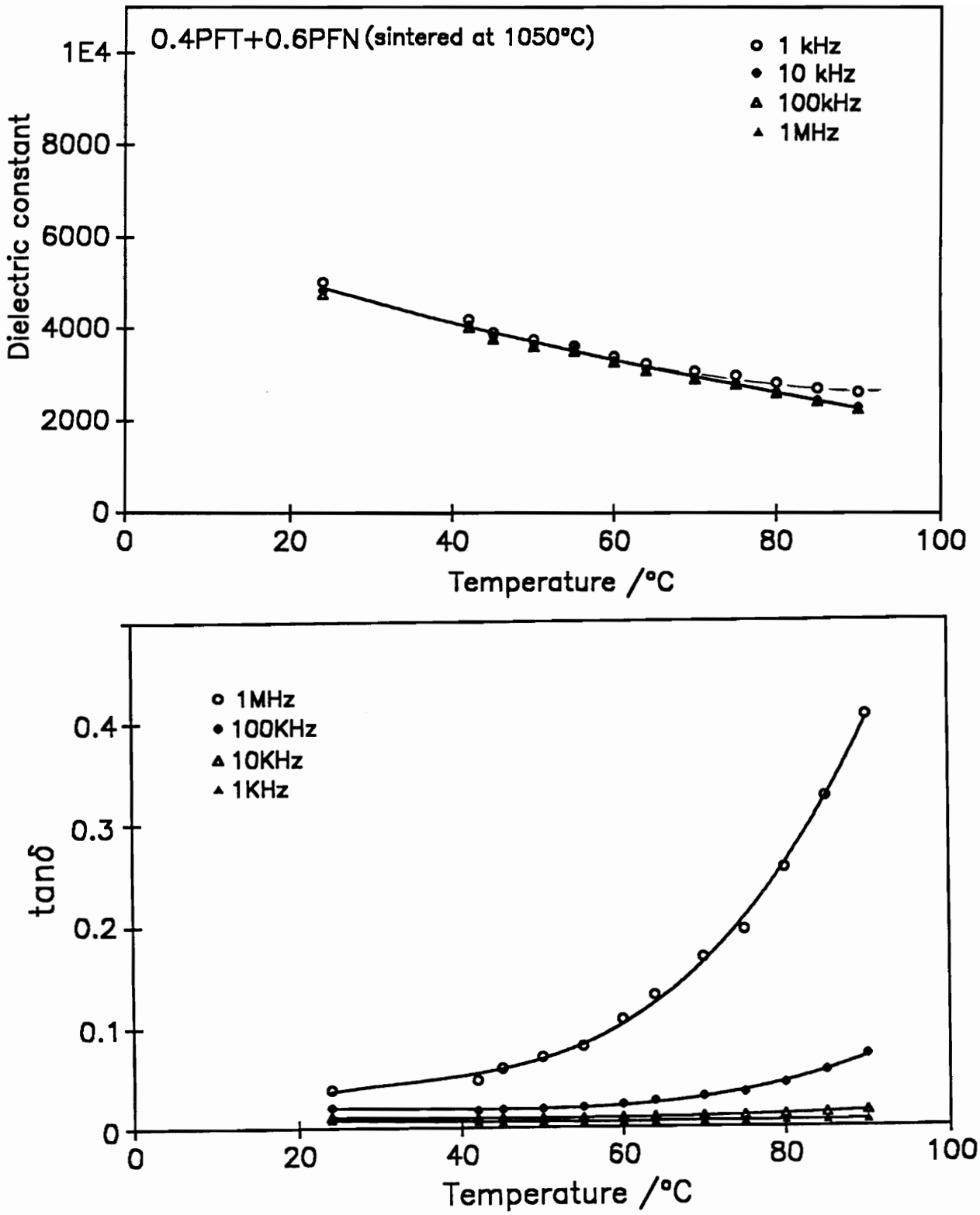

Fig.10 Dielectric property of sample 3 (0.6PFN+0.4PFT synthesized at 800°C) sintered at 1050°C.

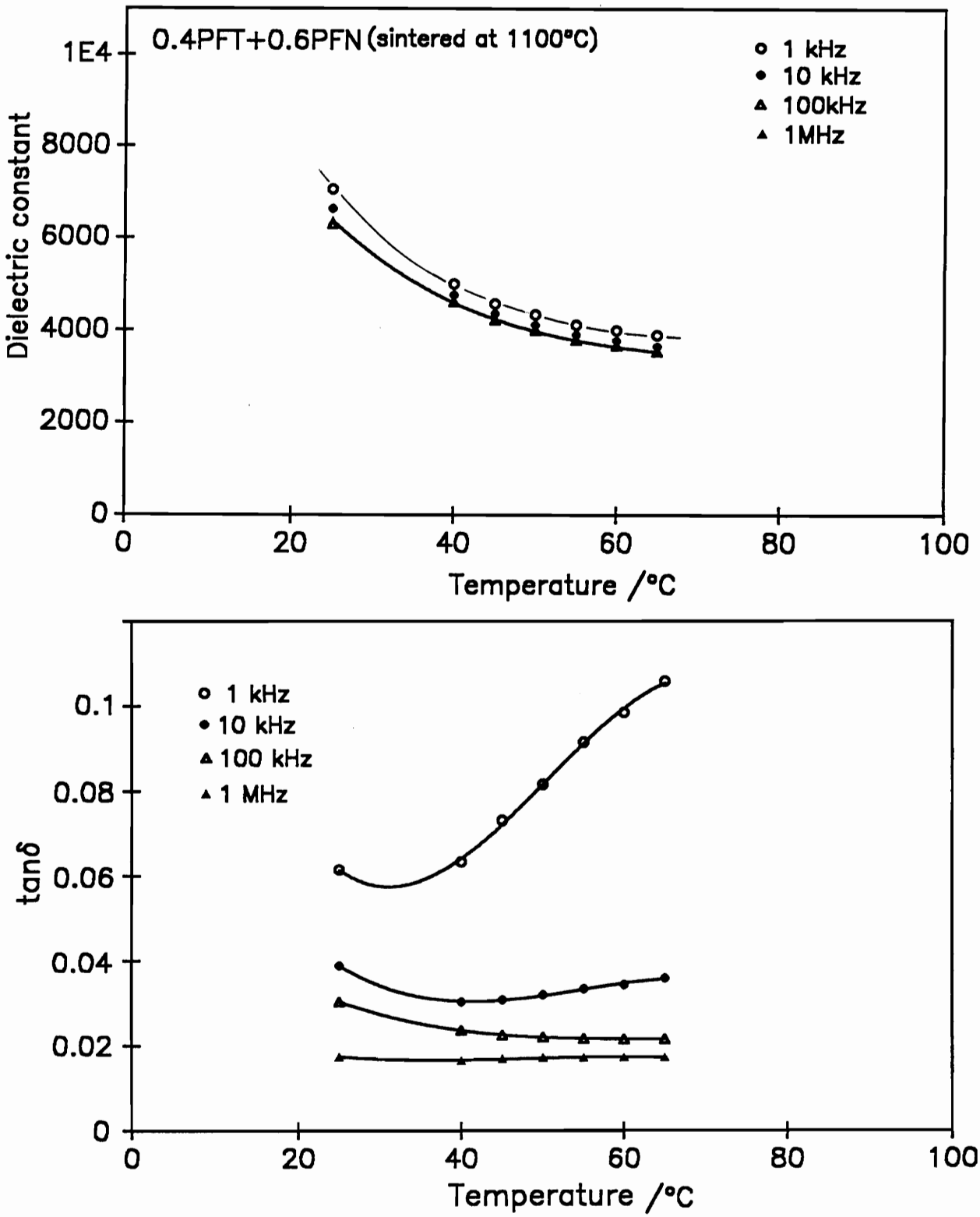

Fig.11 Dielectric property of sample 3 (0.6PFN+0.4PFT synthesized at 800 °C) sintered at 1100 °C.

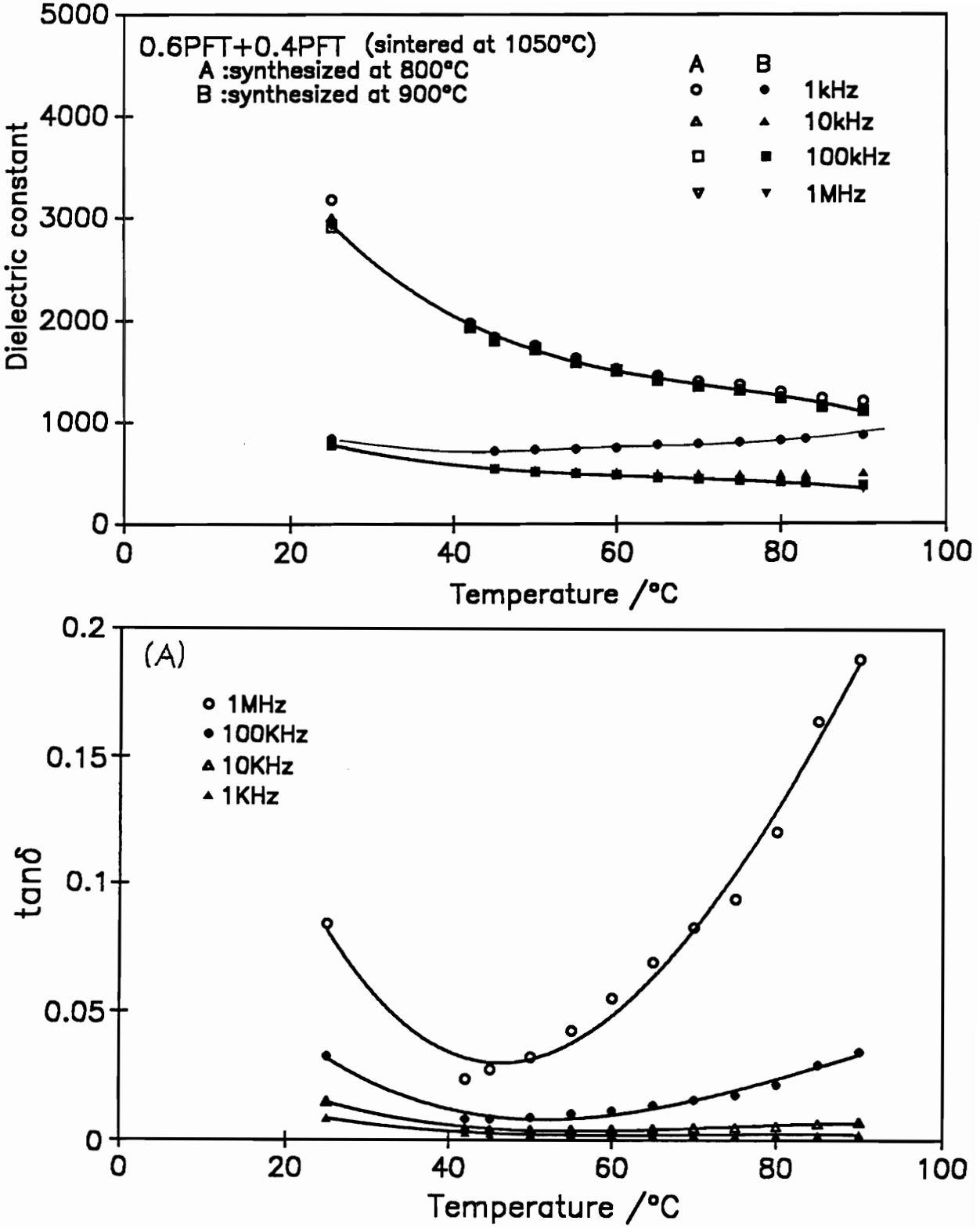

Fig.12 Dielectric constant of sample 4 (0.4PFN+0.6PFT) sintered at 1050°C.

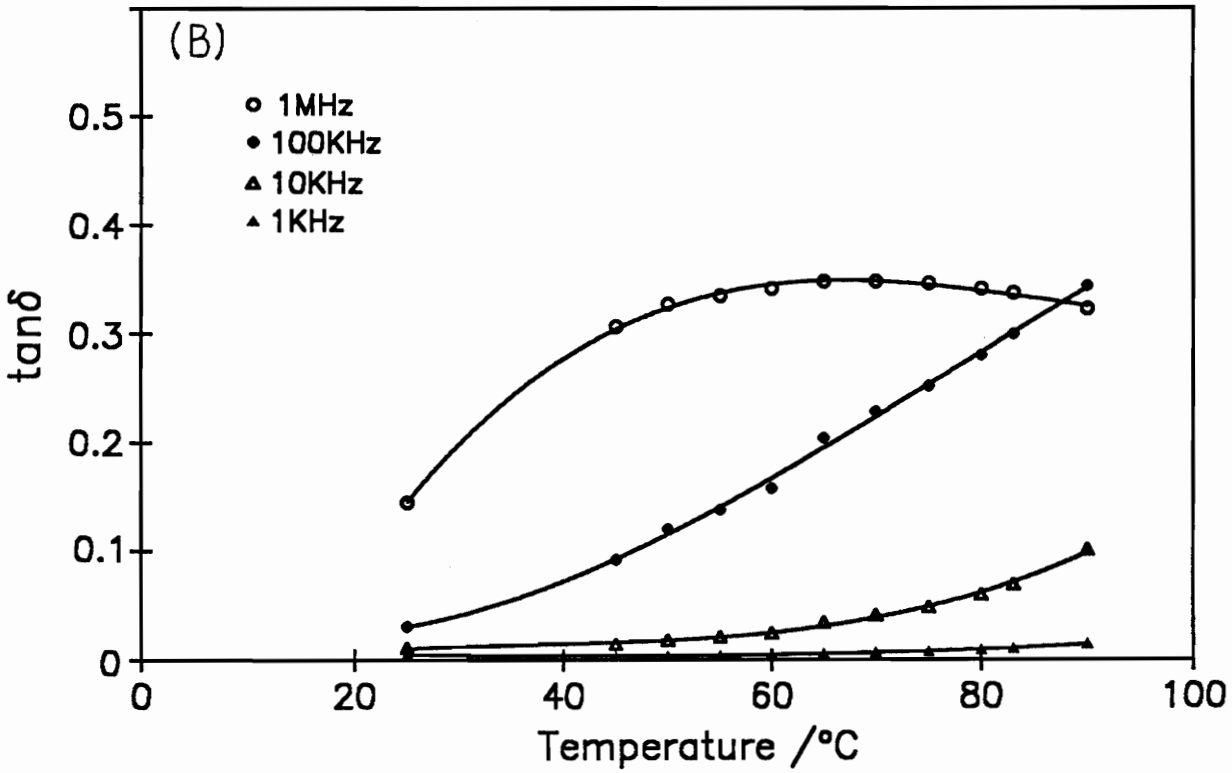

Fig. 12 Continued

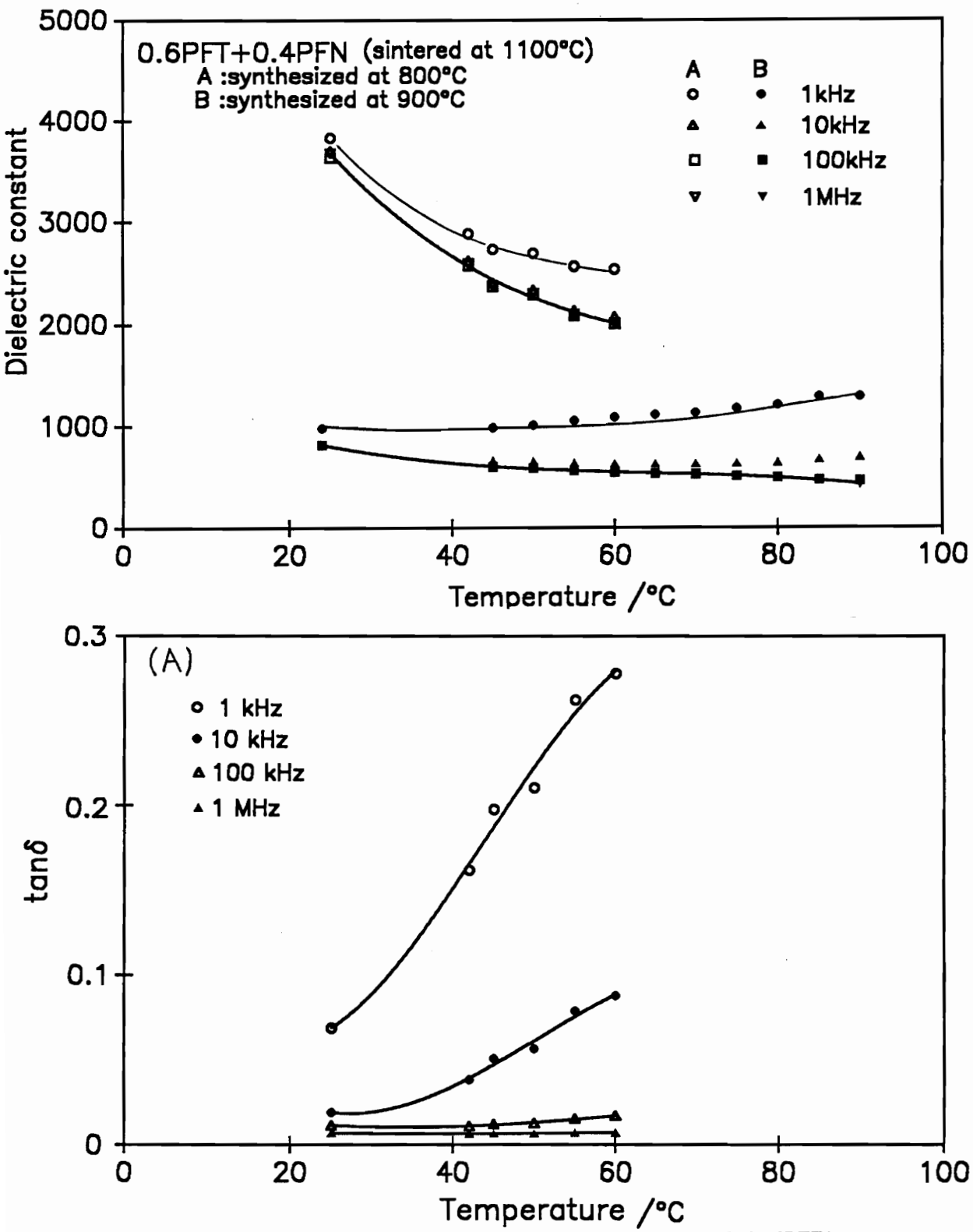

Fig.13 Dielectric property of Sample 4 (0.4PFN+0.6PFT) sintered at 1100°C.

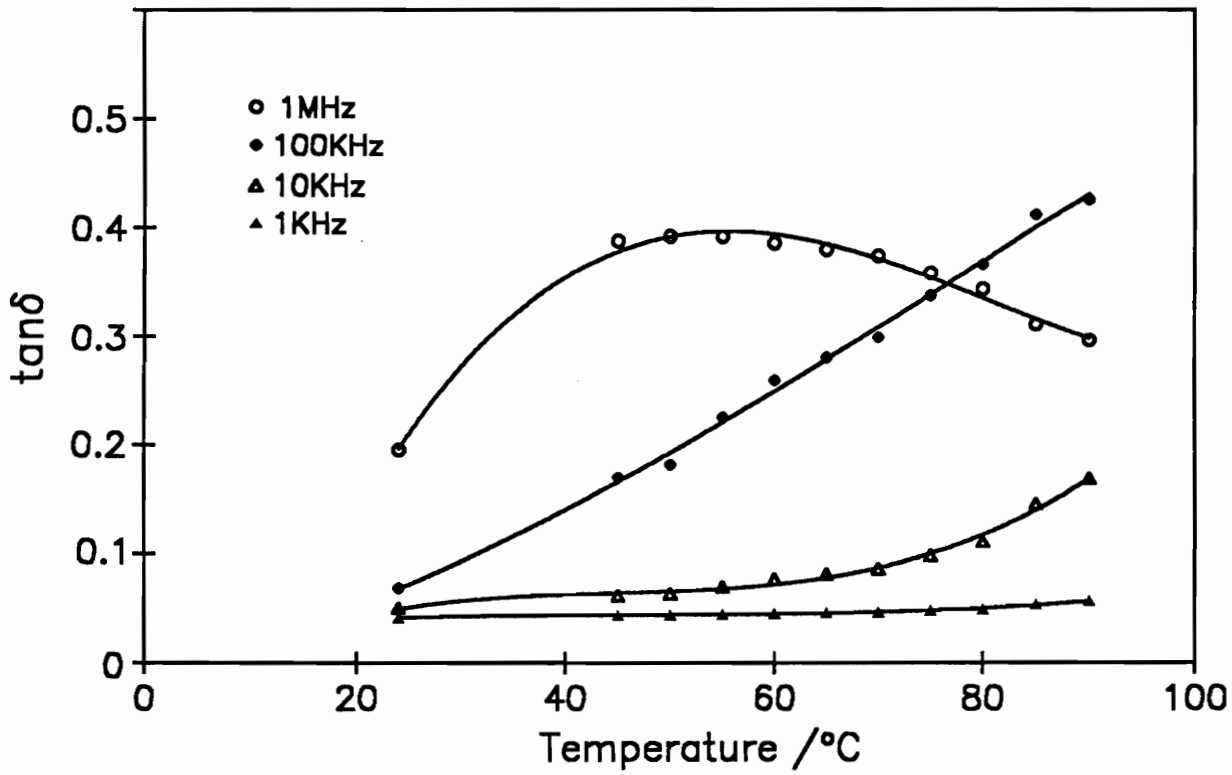

Fig.13 Continued

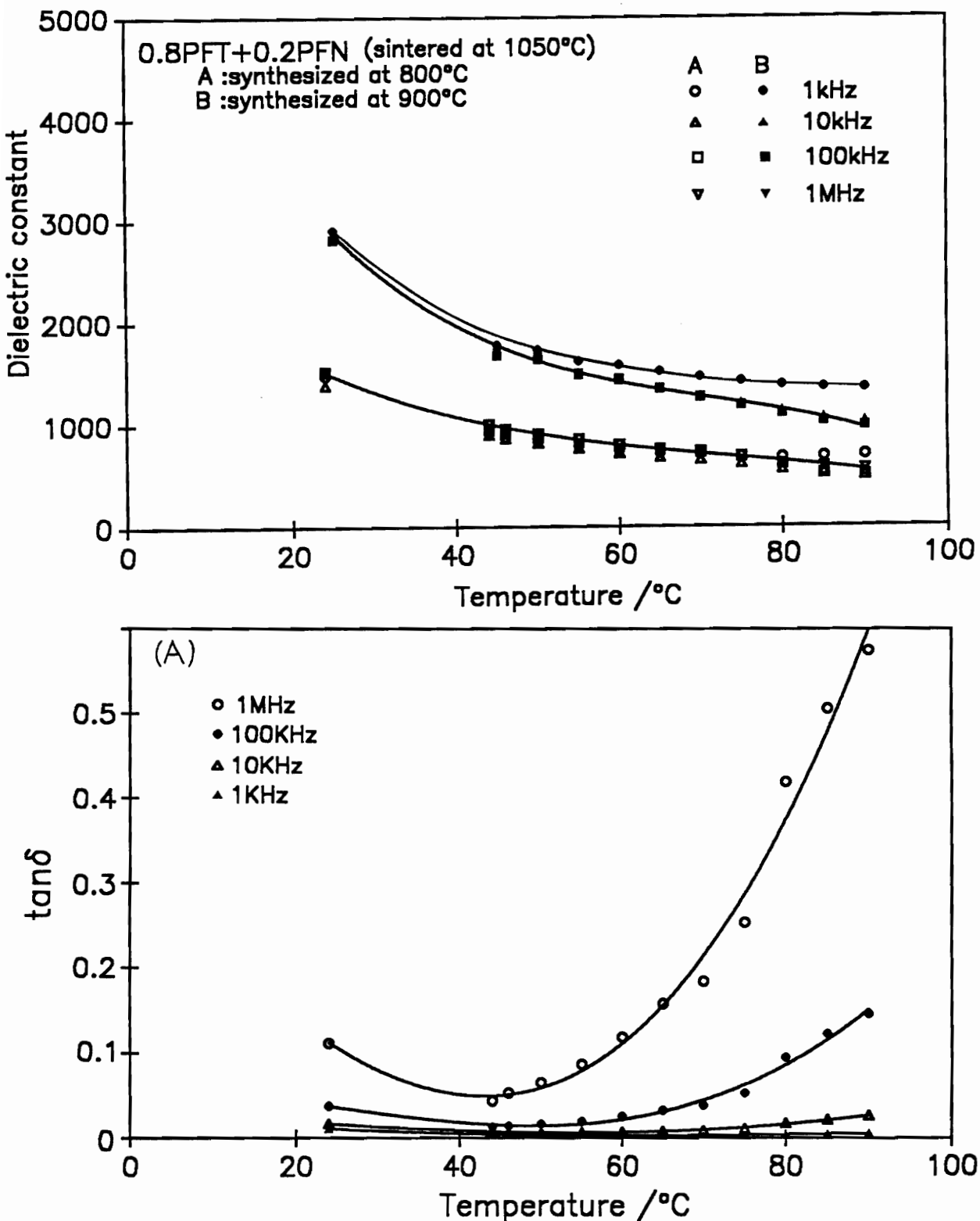

Fig.14 Dielectric property of sample 5 (0.2PFN+0.8PFT) sintered at 1050°C.

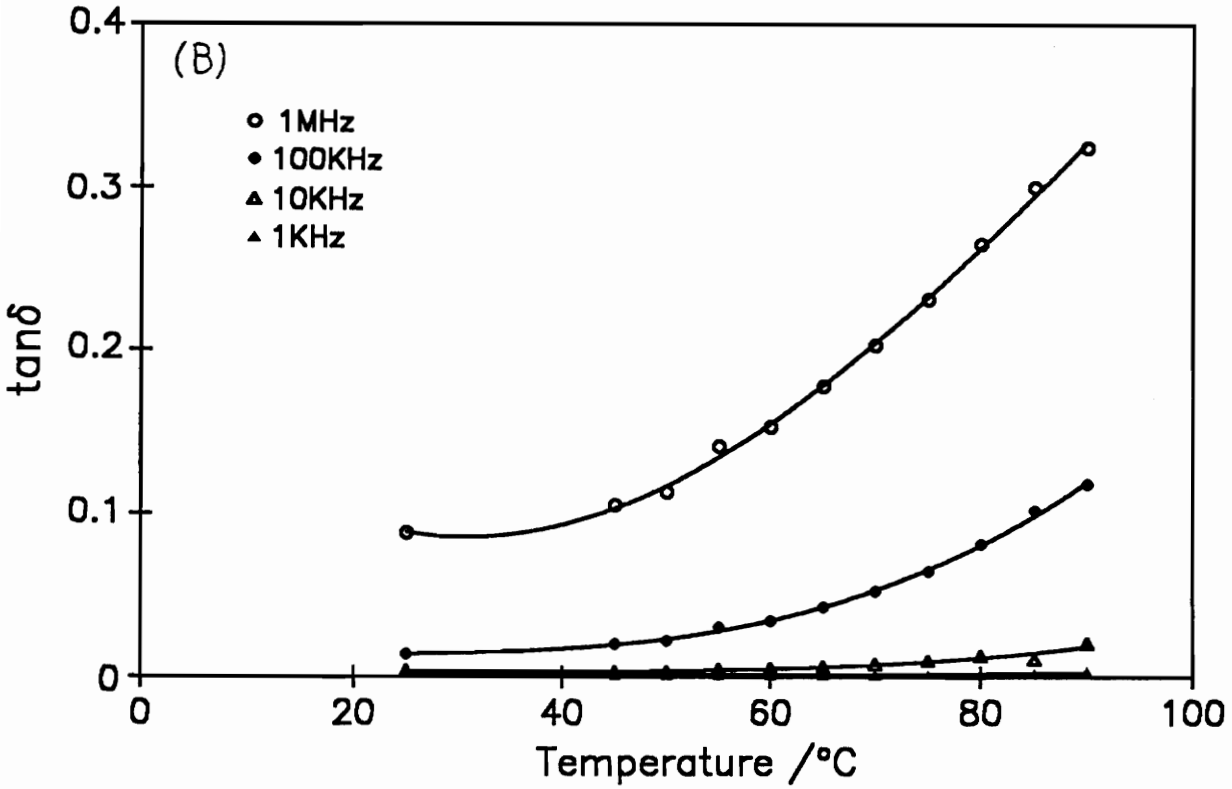

Fig.14 Continued

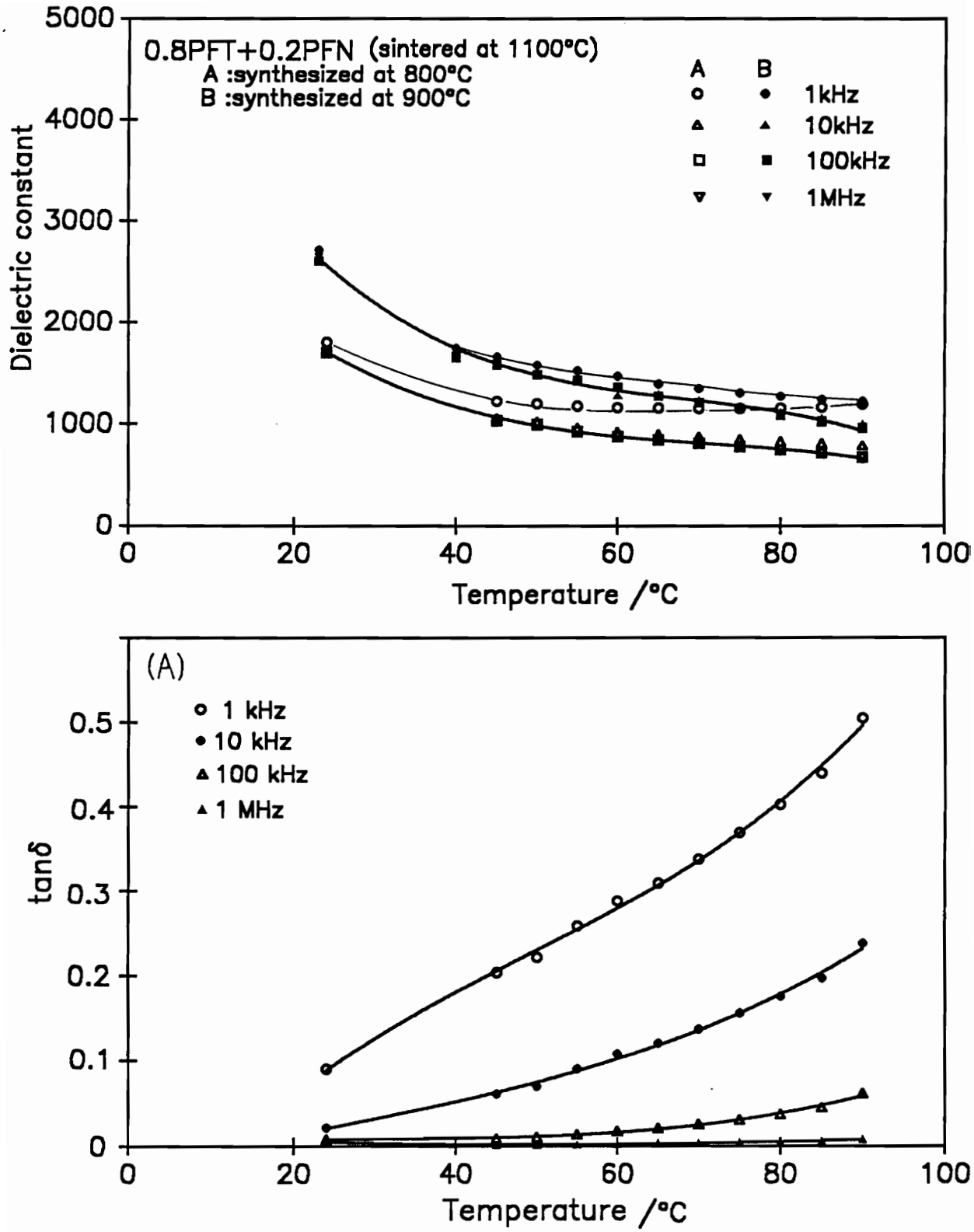

Fig.15 Dielectric property of sample 5 (0.2PFN+0.8PFT) sintered at 1100°C.

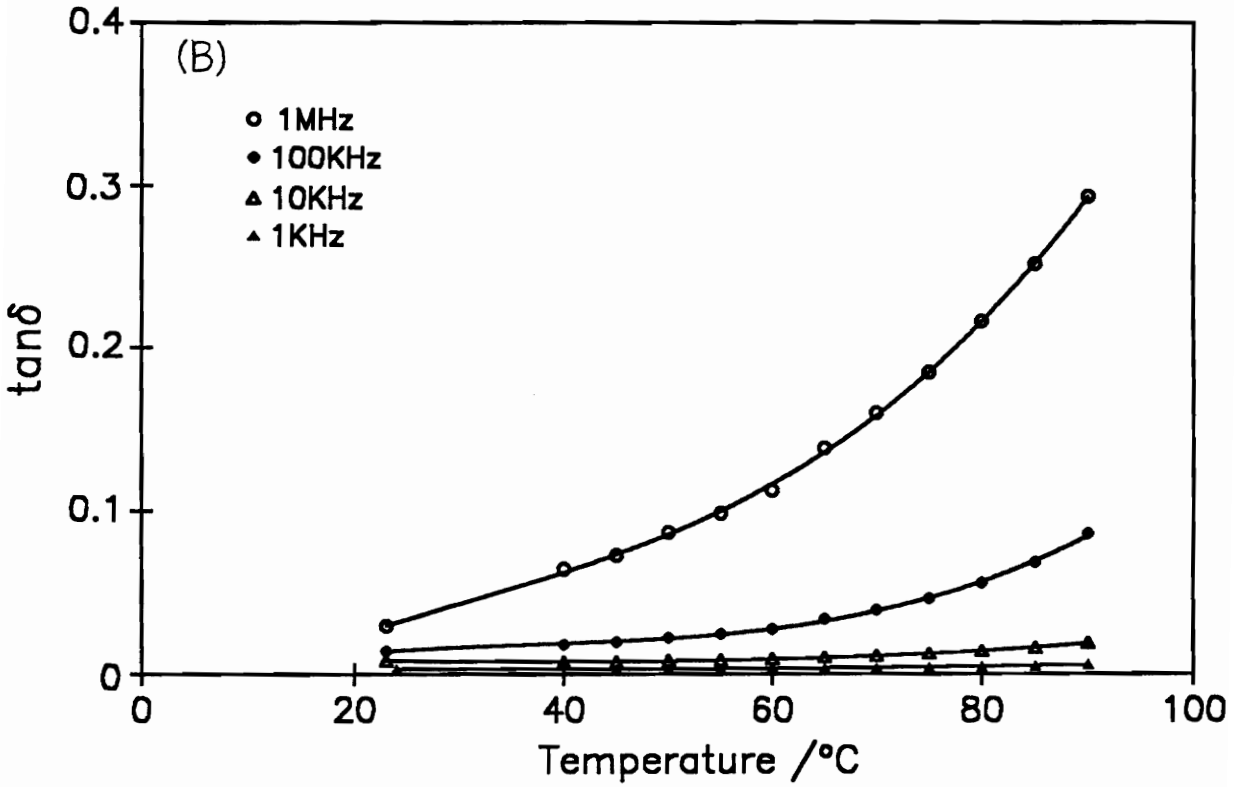

Fig. 15 Continued

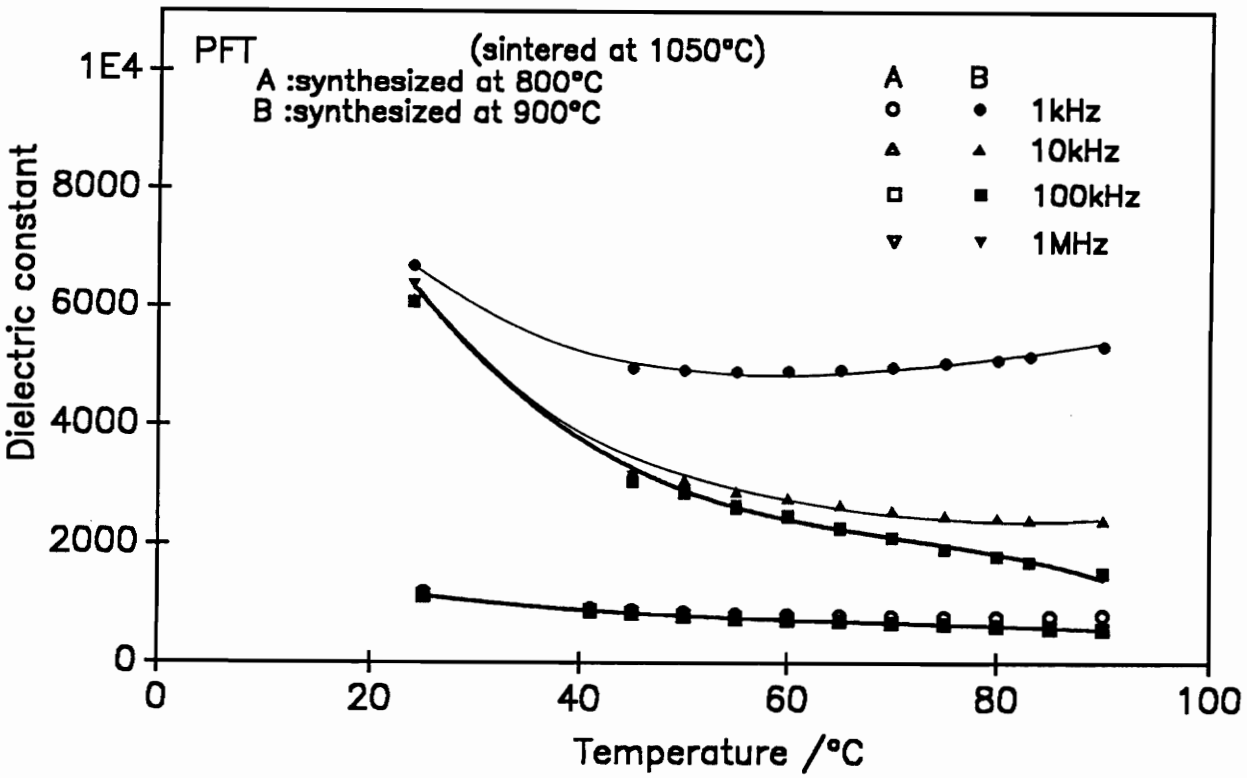

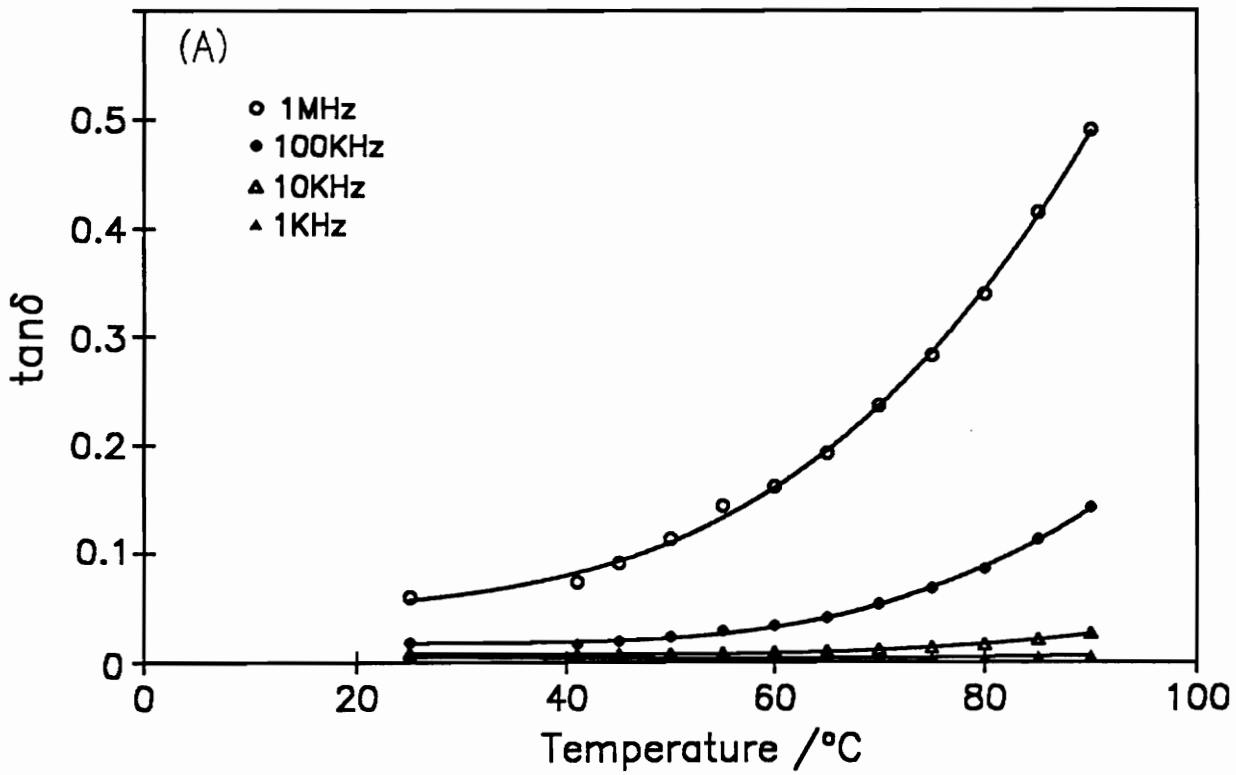

Fig.16 Dielectric property of sample 6 (PFT) sintered at 1050°C.

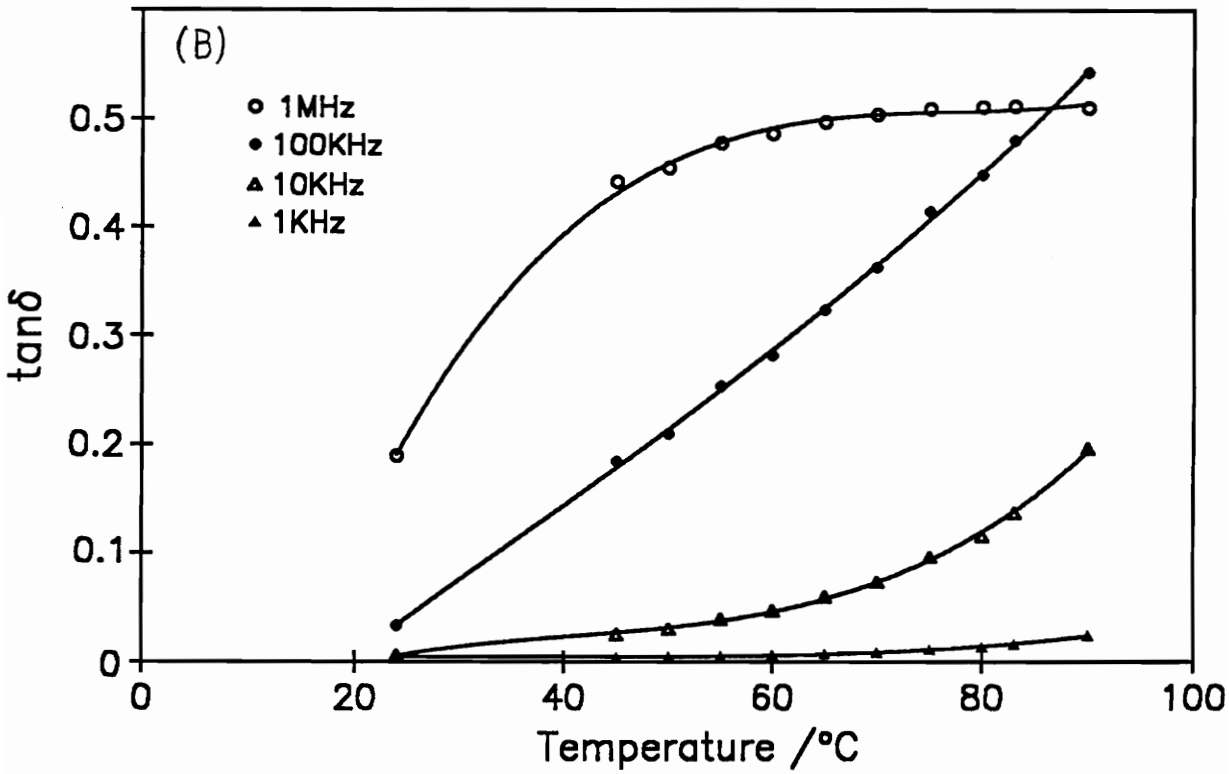

Fig.16 Continued

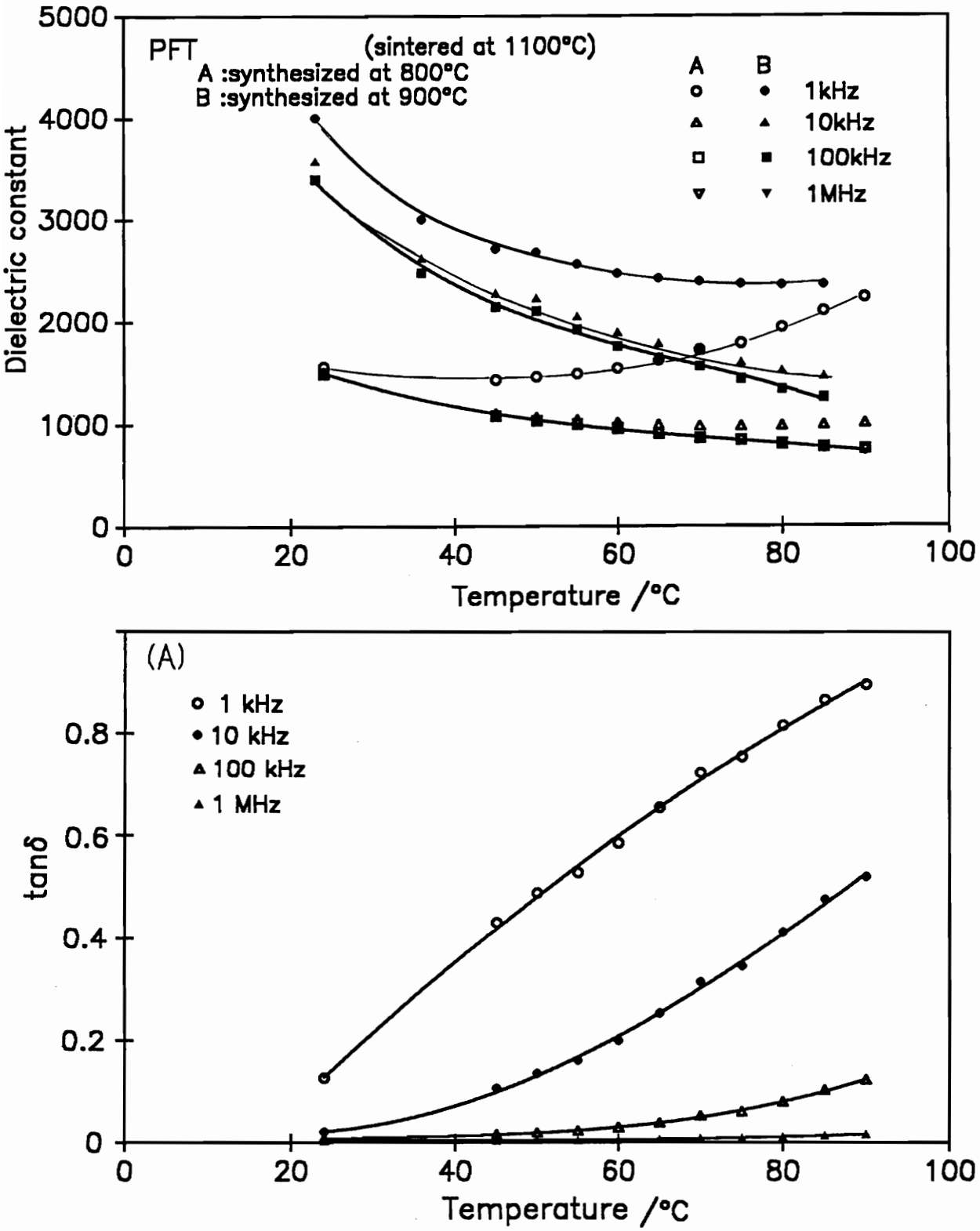

Fig.17 Dielectric property of sample 6 (PFN) sintered at 1100°C.

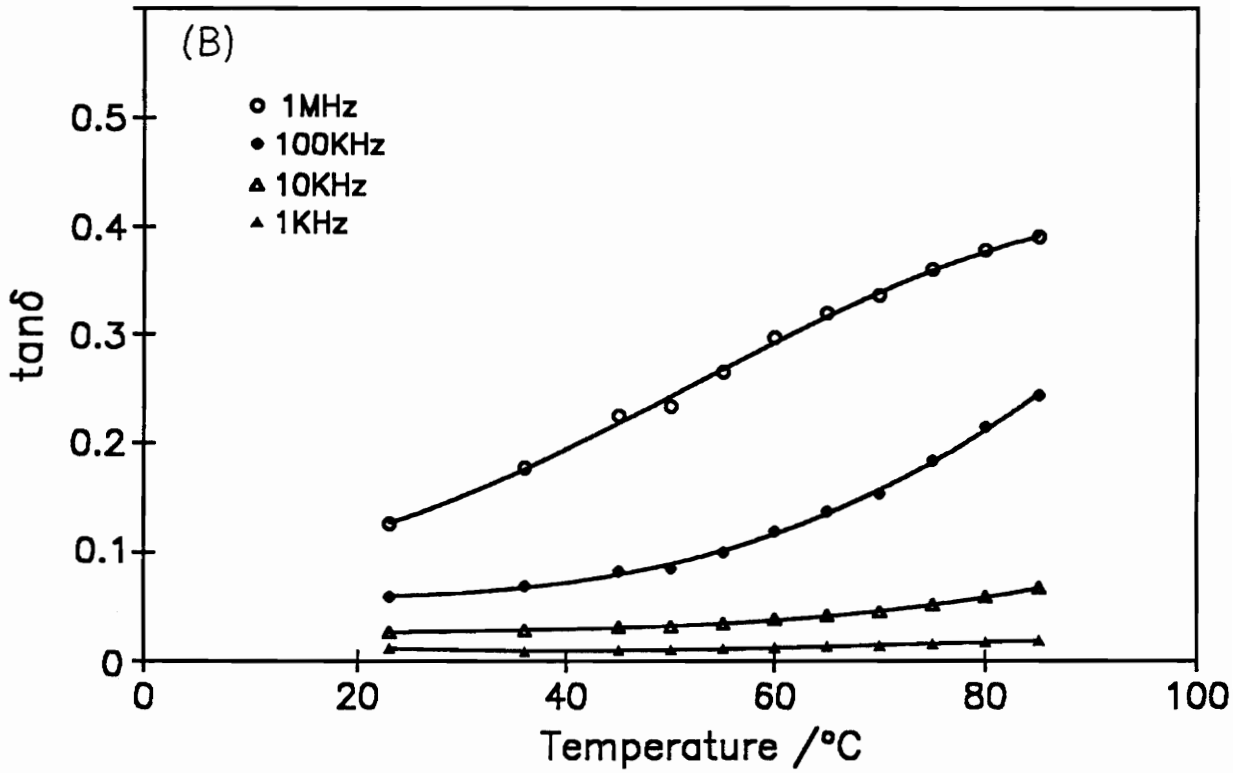

Fig.17 Continued

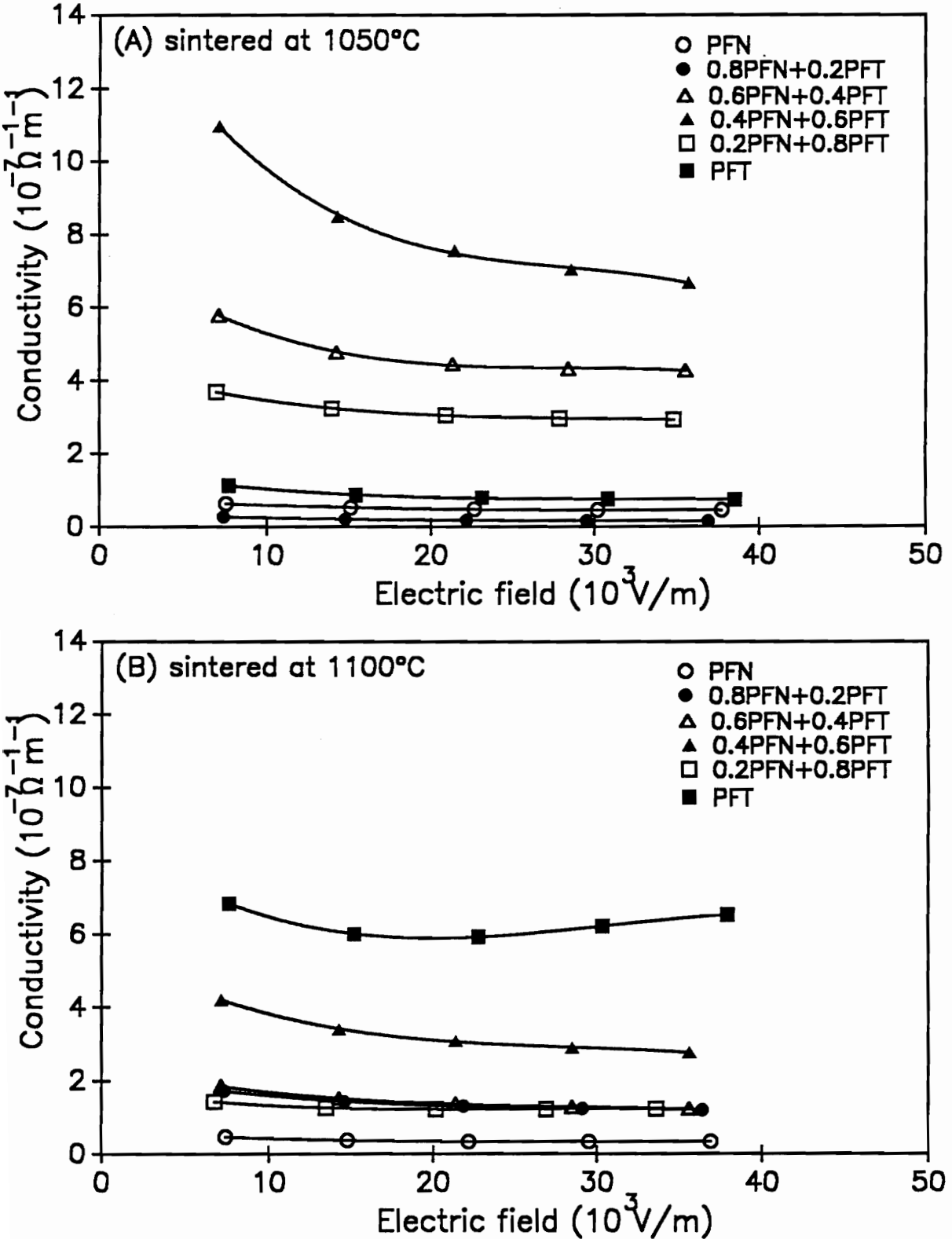

Fig.18 DC conductivity od samples synthesized at 800°C (A) sintered at 1050°C, (B) at 1100°C.

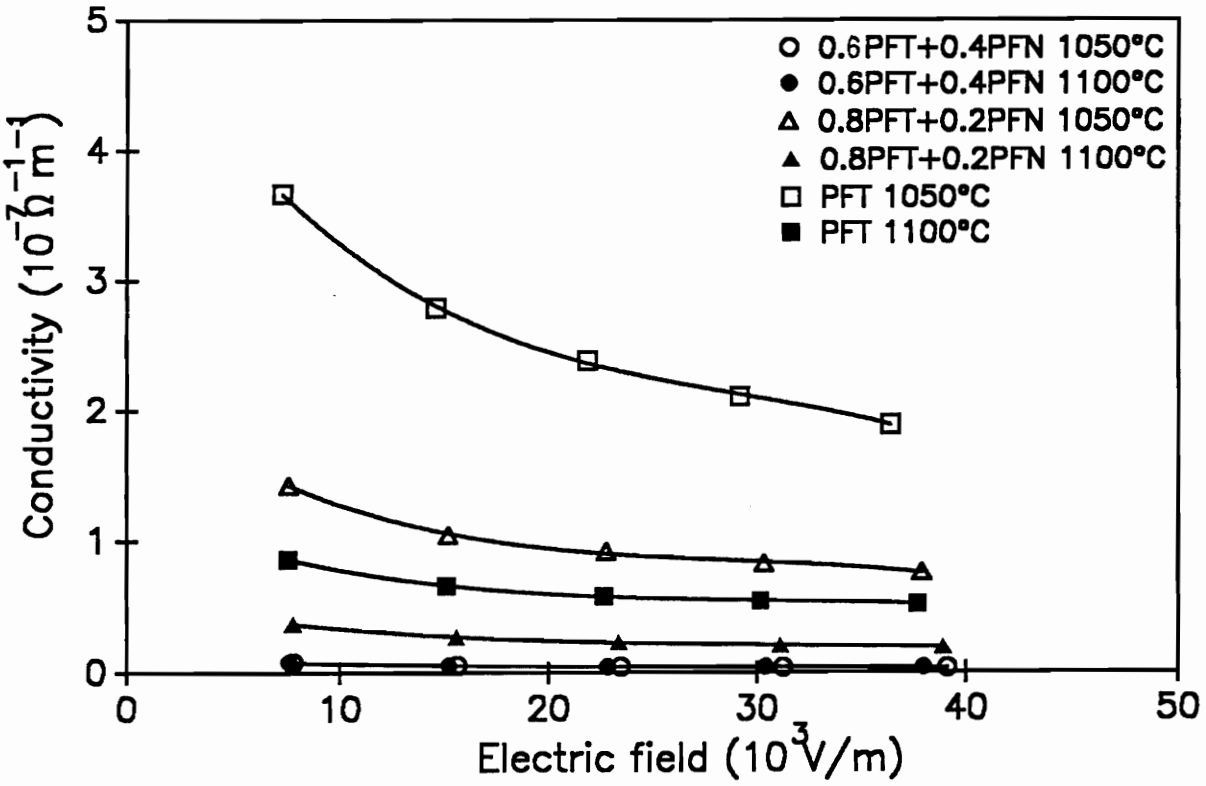

Fig.19 DC conductivity of samples synthesized at 900°C.

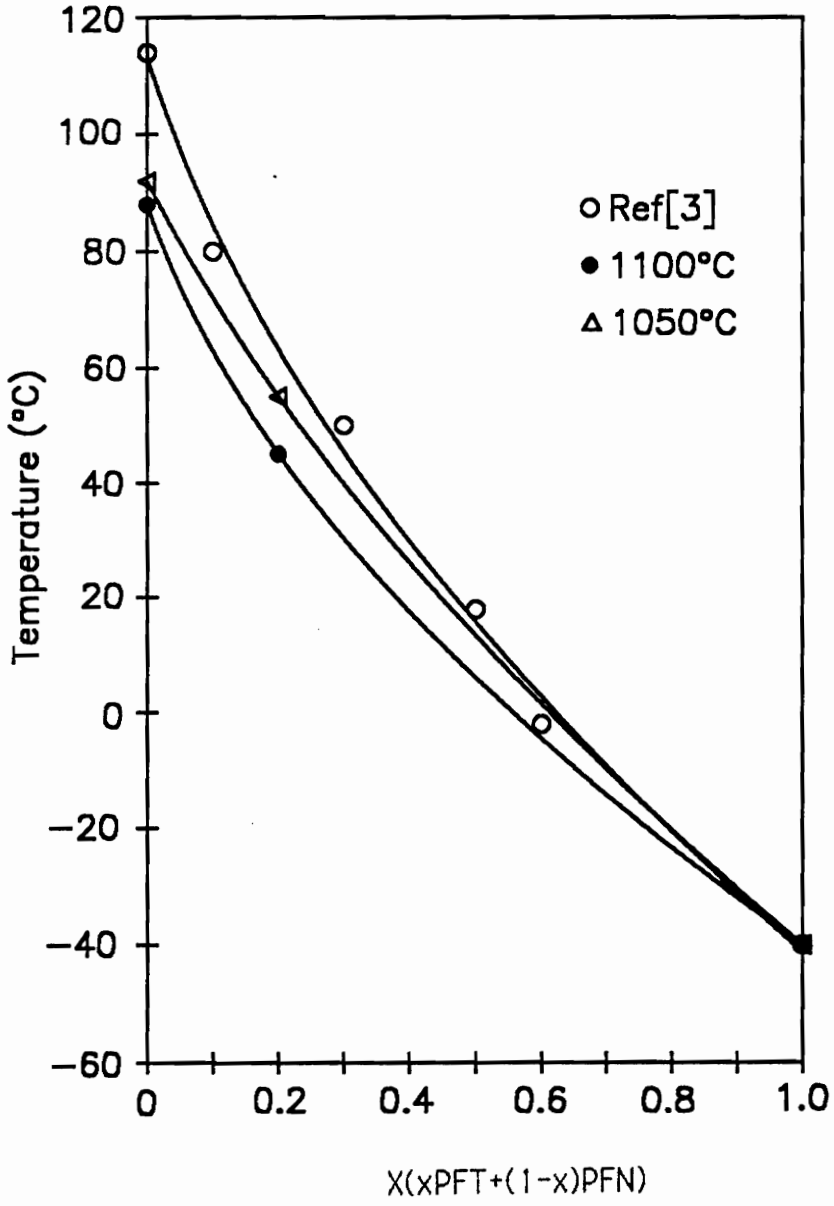

Fig.20 Curie Temperature

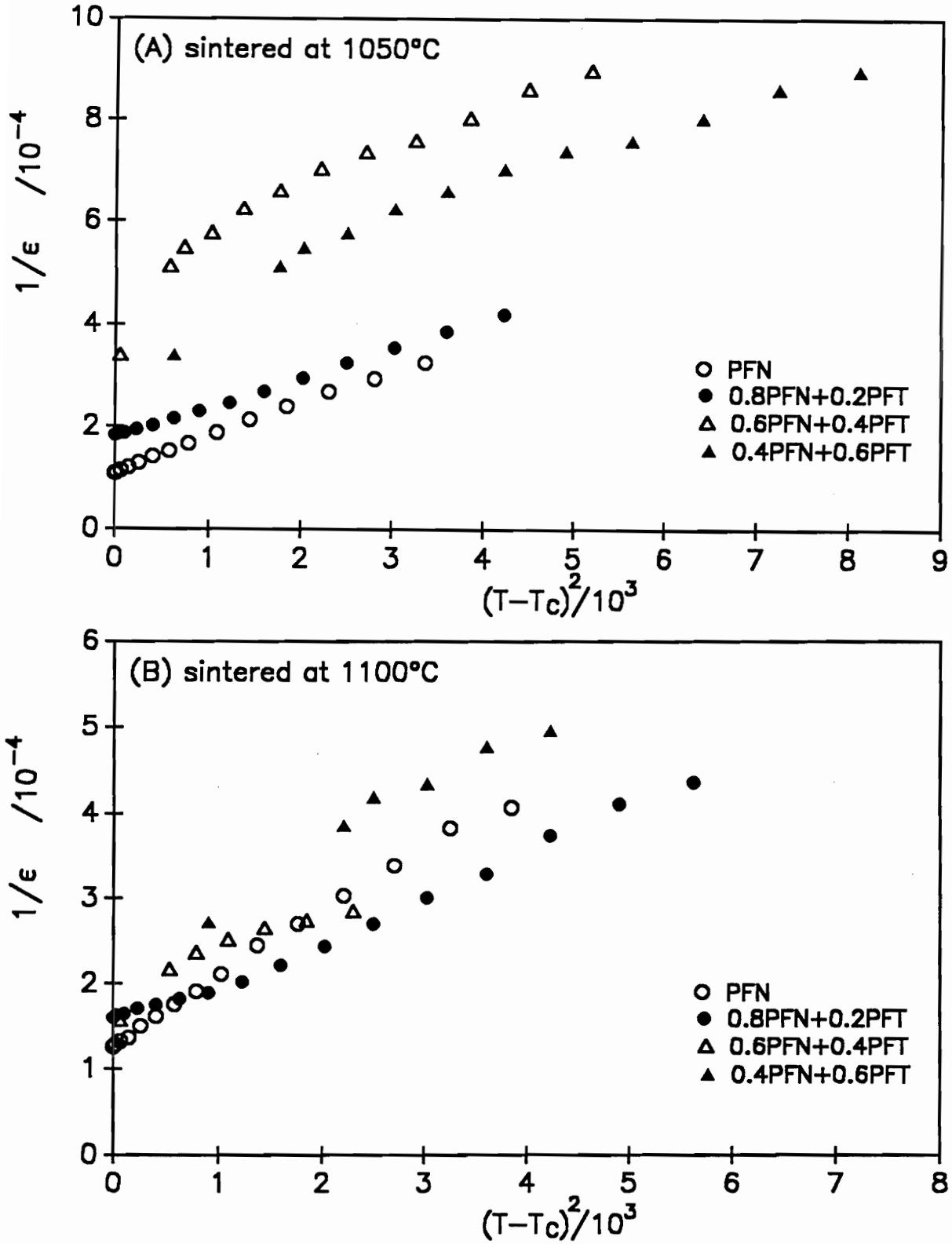

Fig.21 1/ε vs. $(T-Tc)^2$ (A) sintered at 1050°C (B) at 1100°C (C) sample 5 and 6.

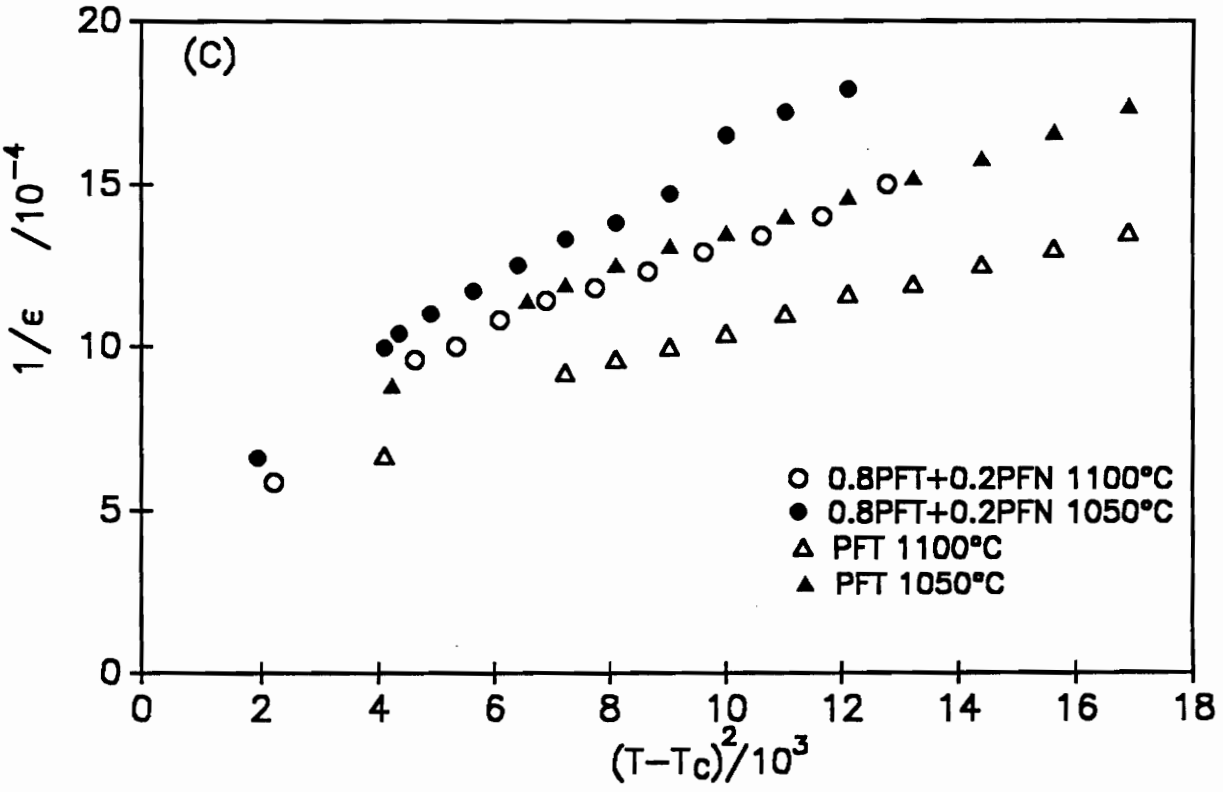

Fig.21 Continued

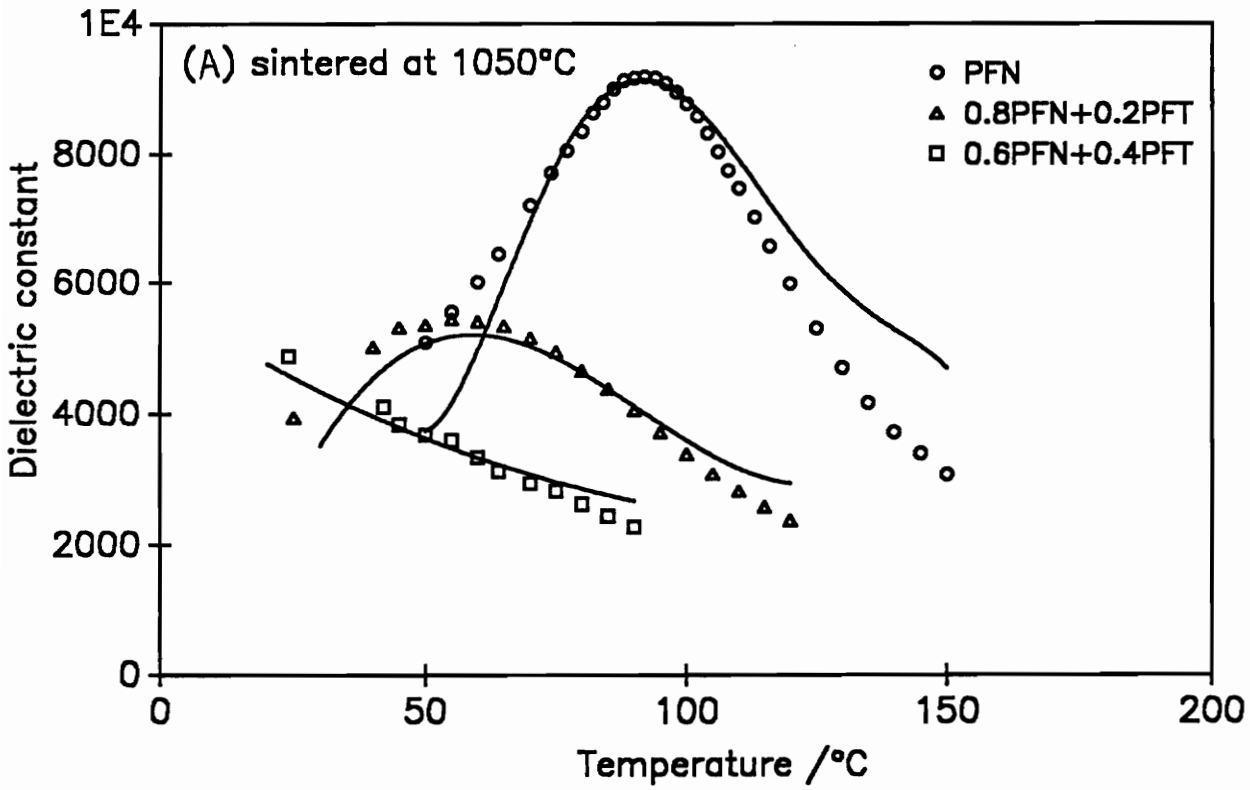

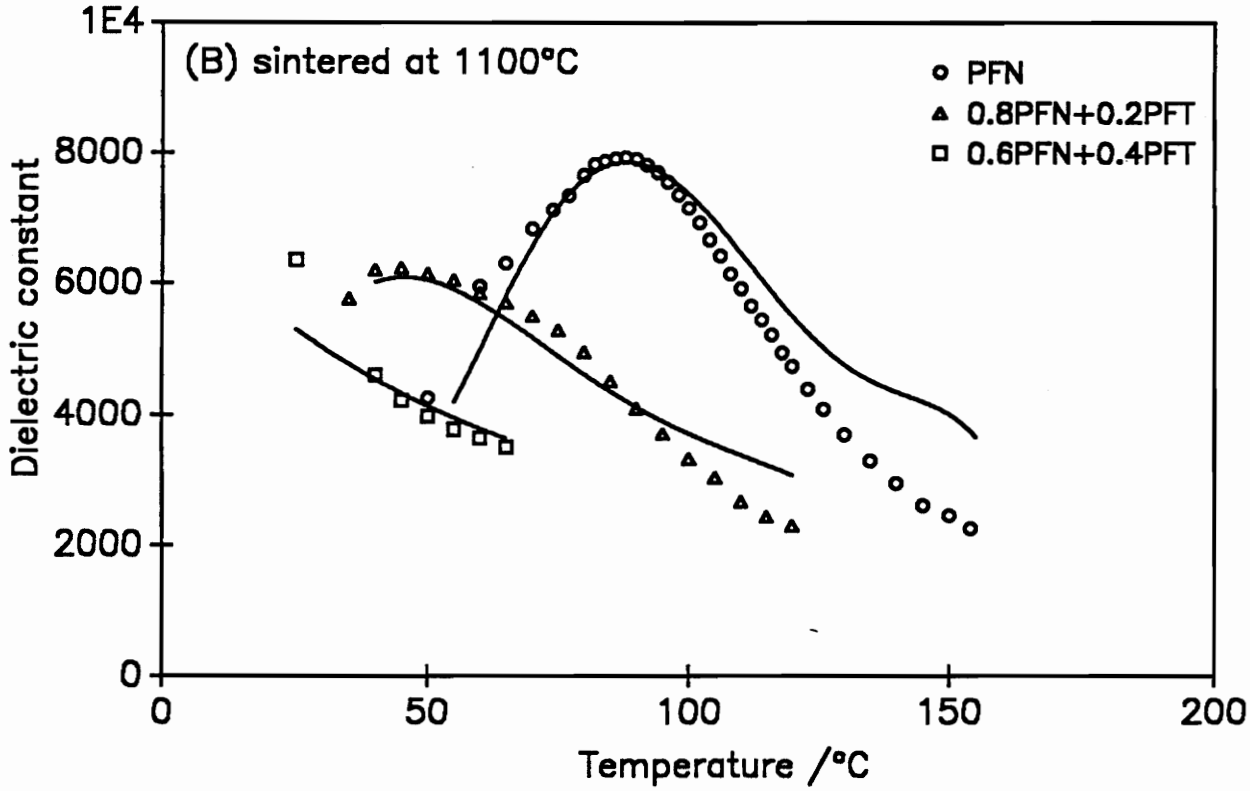

Fig.22 Calculated dielectric constant (A) sintered at 1050°C, (B) at 1100°C.